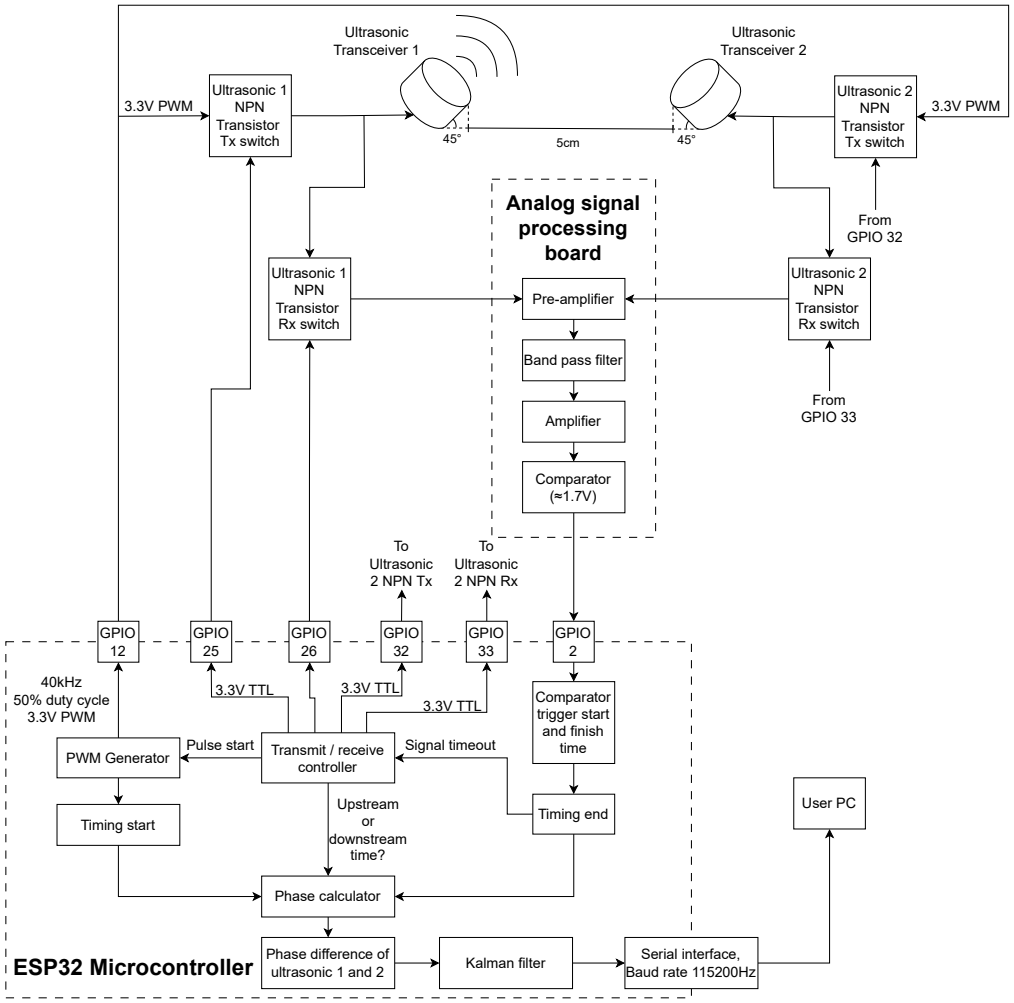

An ultrasonic anemometer for lightweight fixed-wing UAV airspeed measurements

Master's thesis in Embedded Electronic System Design

JOSHUA GERAGHTY

DEPARTMENT OF MICROTECHNOLOGY AND NANOSCIENCE
CHALMERS UNIVERSITY OF TECHNOLOGY
Gothenburg, Sweden 2025
www.chalmers.se

Master's thesis 2025

An ultrasonic anemometer for lightweight fixed-wing UAV airspeed measurements

JOSHUA GERAGHTY

CHALMERS
UNIVERSITY OF TECHNOLOGY

Department of Microtechology and Nanoscience
Chalmers University of Technology
Gothenburg, Sweden 2025

An ultrasonic anemometer for lightweight fixed-wing UAV airspeed measurements
Joshua Geraghty

Supervisor: Lars Svensson, Department of Microtechnology and Nanoscience
Company supervisor: Fredrik Falkman, Sjöräddningssällskapet
Examiner: Per Larsson-Edefors, Department of Microtechnology and Nanoscience

Master's Thesis 2025
Department of Microtechnology and Nanoscience
Chalmers University of Technology
SE-412 96 Gothenburg
Telephone +46 31 772 1000

Cover: Ultrasonic airspeed sensor system overview block diagram

Typeset in LaTeX
Gothenburg, Sweden 2025

An ultrasonic anemometer for lightweight fixed-wing UAV airspeed measurements
Joshua Geraghty
Department of Microtechnology and Nanoscience
Chalmers University of Technology

Abstract

This thesis explores the development of an ultrasonic airspeed sensor for lightweight fixed-wing drones. The ultrasonic airspeed sensor acts as an alternative to Pitot-static systems, a differential pressure sensor used for obtaining airspeed data for aircraft. The design takes inspiration from commercially available ultrasonic anemometers and ultrasonic distance sensors.

The prototype consists of two ultrasonic transceivers facing each other at a predefined distance. One ultrasonic transceiver will transmit a signal, while the other will receive it. These roles will change to obtain an upstream and downstream airspeed measurement. The system records the time of initial transmission to receiving the signal, and by knowing the distance between the two ultrasonic sensors, the speed of sound can be established. Many factors can influence the speed of sound, however the only factor that has a directional component is wind. Taking advantage of this, the influence of wind and all other atmospheric conditions on the speed of sound can be separated.

The ultrasonic signal is processed by an analog signal conditioning circuit consisting of amplifiers, filters and a comparator. A received ultrasonic signal peak is detected by the transition of comparator states, which is used to determine the transmission time. Cross-correlating upwind and downwind signal phases will determine the indicated airspeed measurement, which requires further calibration to obtain calibrated airspeed measurements.

Keywords: airspeed measurements, Pitot-static systems, signal processing, ultrasonic transceivers, ultrasonic anemometers, digital signal processing, transit-time

Acknowledgements

I would like to thank my advisors Fredrik Falkman and Lars Svensson for the opportunity to develop this thesis. The support provided by both advisors has been invaluable, and this project would not have been possible without their advice and encouragement.

I am grateful for those at the CASE Lab and ETA for providing me with the resources necessary to complete this project. Many a long day has been spent in their facilities, and their hospitality and advice is well appreciated.

I would like to thank Isak Jonsson, Arion Pons, Patxi Rodriguez Acero, Daniel Poveda Pi and all at the Fluid Dynamics department at Chalmers for allowing me to test the ultrasonic airspeed sensor in the wind tunnel, and providing initial advice on the project.

The communication of an idea is just as valuable as the idea itself. I would like to thank Per Larsson-Edefors for his guidance on creating a report that can be well understood by future developers of this thesis.

Lastly, I'd like to extend my appreciation to my family, friends, and my girlfriend Astrid for providing me with the encouragement to complete this project. Their love and support always made me feel confident in my abilities to complete this project.

Joshua Geraghty, Gothenburg, June 2025

List of Acronyms

Below is the list of acronyms that have been used throughout this thesis listed in alphabetical order:

1D	One-dimensional
AC	Alternating Current
ADC	Analog to Digital Converter
AI	Artificial Intelligence
CANBUS	Controlled Area Network Bus
DC	Direct Current
EMC	Electromagnetic Compatibility
EMI	Electromagnetic Inteference
FIR	Finite Impulse Response
FPGA	Field Programmable Gate Array
GPS	Ground Position System
GUM	Guide to the Expression of Uncertainty in Measurement
I2C	Inter-Integrated Circuit
IC	Integrated Circuit
IIR	Infinite Impulse Response
IP Rating	Ingress Protection Rating
OTP	One Time Programming
PCB	Printed Circuit Board
PWM	Pulse Width Modulation
SPI	Serial Peripheral Interface
SSRS	Swedish Sea Rescue Society
TTL	Transistor-Transistor Logic
UAV	Uncrewed Aerial Vehicle

Contents

List of Figures

1

Introduction

The relative velocity of an object to the air is known as airspeed. This quantity is essential to generate lift in an aircraft, which is a force that directly opposes the weight of an aircraft and holds the aircraft in the air. An airspeed measurement is composed of two relative velocities, the ground speed and wind speed. The ground speed is the measurement of aircraft movement in reference to the ground, while the wind speed is the movement of air in reference to the ground. On a perfectly calm day, the ground speed is equal to the airspeed. Wind speed will either increase or decrease the ground speed, depending on the direction of travel relative to each other. This difference will equate to the airspeed of the object.

Air has a variety of properties which can be accounted for to obtain more accurate airspeed measurements. Four different types of airspeeds exist [1]:

- Indicated airspeed, which is read directly from airspeed measurement tools.
- Calibrated airspeed, which is corrected for position installation and instrument errors.
- Equivalent airspeed, which uses calibrated airspeed measurements, and corrects the value to account for air compressibility.
- True airspeed, which uses calibrated airspeed measurements, and corrects the value for altitude and temperature.

Each airspeed type has specific use cases, however the most used airspeeds are indicated airspeed and true airspeed. For aircraft, the most common wind speed systems are Pitot-static systems, a differential pressure system. The indicated airspeed of an aircraft can be obtained by using Pitot-static system wind speed measurements in combination with GPS ground speed data. By processing the indicated airspeed further using altimeters, thermometers and position correction systems, the true airspeed can be determined.

This project is developed in collaboration with Swedish Sea Rescue Society (SSRS), a voluntary sea rescue organisation based in Sweden [2]. The Swedish Sea Rescue Society is working on a new type of fixed-wing drone, that will be stationed along the Swedish coast. The purpose of the drone is to fly to accident locations and provide rescue personnel with information about the accident before they arrive at the scene. The current design uses a Pitot-static system for airspeed measurements, however Pitot-static systems are vulnerable to water blockages within its tubing system. The drone is expected to fly in bad weather conditions, therefore an alternative airspeed measurement device is required.

1.1 Aim and Scope

The main purpose of this thesis is to develop a prototype low-cost ultrasonic based airspeed sensor for a fixed-wing drone, and analyse the system performance compared to commercially available Pitot tubes airspeed systems. The ultrasonic airspeed sensor will take inspiration from ultrasonic anemometer designs. The purpose of the ultrasonic airspeed sensor is to provide a middle ground between the accuracy of ultrasonic anemometers, and low power performance of ultrasonic distance sensors. The goal of this thesis is to provide an ultrasonic airspeed sensor with a measurement resolution of ± 0.25m/s, measurement range of 0m/s to 30m/s, and a minimum output rate of 20Hz.

1.2 Limitations

This section considers aspects of the project which are relevant, however outside of the scope of this project.

1.2.1 Transmission medium characteristics

The ultrasonic airspeed sensor is designed to propagate through air, however humidity, temperature and the chemical composition of air will influence the speed of sound through the medium. The ultrasonic airspeed sensor will be tested within a controlled environment, therefore the effects of the following medium characteristics will not be considered during testing:

- Acoustic performance within mediums containing high water vapour, such as fog, mist or humid air.
- Sensor performance with temperature differences. The sensor will be tested within room temperatures of 20°C to 22°C.
- Performance of sensor due to alterations within the air chemical composition e.g. exhaust fumes.

The ultrasonic airspeed sensor will be designed to account for these changing conditions, however creating these conditions within a controlled testing environment will not be possible within the given time frame. Outdoor testing without attaching the device to a drone is possible, but will not reflect true operation of the device.

1.2.2 Sensor characteristics

The main performance characteristics that will be considered are airspeed accuracy, power usage, weight and size. These factors will be compared to commercially available airspeed and wind speed sensors, such as Pitot tubes and ultrasonic anemometers.

The thesis will not evaluate the following sensor aspects:

- Electromagnetic Compatibility (EMC) and Electromagnetic Interference (EMI) of the ultrasonic airspeed sensor.
- Weathering of the ultrasonic airspeed sensor, and determining an IP rating for the device.

- Lifespan of error free ultrasonic airspeed sensor operation.
- Evaluation of uncertainty as outlined within the Guide to the Expression of Uncertainty in Measurement, commonly known as the GUM [3].

1.2.3 Drone integration

The ultrasonic airspeed sensor will be developed as a stand-alone, prototype system. This means that the sensor will not be integrated into the overall drone system, and therefore flight testing cannot be performed.

The thesis will not evaluate the following aspects:

- Development of an ultrasonic airspeed sensor which is fully compatible with ArduPilot. ArduPilot integration will be considered within the design, however full integration for flight testing is outside of the project scope.
- Ultrasonic airspeed sensor performance comparison to Pitot tubes during flight testing.
- Ultrasonic airspeed sensor performance comparison during harsh weather conditions, including heavy rain, fog and extreme cold.
- Effects of sensor integration on drone power consumption and battery life. The sensor system power usage as a stand-alone product will be considered. Calculations to determine the effects of sensor integration on the overall drone battery life will be completed, however it will not be tested.
- Effects of drone integration on ultrasonic airspeed sensor performance, caused by drone vibrations or electromagnetic interference from motor control units.

1.3 Related work

The usage of ultrasonic signals to record the velocity of a gas or liquid is well established, with applications for wastewater flow measurements [4], airflow measurement devices for ducted air, and oil flow. These devices provide the advantage of requiring minimal maintenance, as the devices do not contain any moving components. If maintenance is required, device deinstallation is simple since the flow meter is non-intrusive, and can be clamped onto pipes and tubing. A typical architecture of ultrasonic flow sensors consists of two ultrasonic transceivers, which are placed non-perpendicular to the flow inside a tube. In conditions where there is no flow, the transit time from upstream and downstream propagations will remain the same. If a flow is present within the tube, the signal transmission time will increase if the ultrasonic signal is propagated downstream, and the signal transmission time will decrease if the ultrasonic signal is propagated upstream. Since the distance between ultrasonic transceivers has not changed, the flow meters show that the speed of sound has been superposed by a flow. Using a differential system, the ultrasonic flow meter can determine the flow of a known substance by using the upstream and downstream transit times.

The ultrasonic flow meter design methodology has been extended to further applications, such as ultrasonic anemometers, a device used to measure wind velocity. The design theory behind ultrasonic anemometers is well established, with patents existing from 1990 [5, 6]. A transceiver pair is required to obtain measurements

within one axis, with up to three pairs used to measure within three axes. Ultrasonic anemometers are becoming more favourable for meteorological studies conducted within harsh weather conditions. The lack of mechanical components makes the ultrasonic anemometer more robust and receptive to quick changes in wind velocity when compared to mechanical anemometers, such as wind vanes or spinning cup anemometers. This type of design has become more popular with the rise of consumer electronics, where ultrasonic anemometers have been developed using an Arduino and HC-SR04 ultrasonic sensors [7, 8].

The repurposing of ultrasonic anemometers as ultrasonic airspeed sensors for uncrewed aerial vehicles (UAVs) has proven successful in recent years. The ultrasonic airspeed sensor presented in [9] uses a two-axis ultrasonic anemometer design. The device was created to allow UAVs with a weight less than 3kg to obtain airspeed readings at velocities below 5m/s with a resolution of 0.1m/s at an output rate of 10Hz. Obtaining all of these characteristics with Pitot tube differential pressure sensors is difficult. The ultrasonic airspeed sensor design is compared to Honeywell's SSCDRRN002ND2A3 differential pressure sensor [10], which has an output rate of 1kHz for analog output values, and 2kHz for digital output values. However, the device cannot measure below 5m/s, as the measurement range is limited to 160Pa to 1MPa. For reference, the dynamic pressure of wind can be determined with Equation 1.1, where q_s is the dynamic pressure, ρ is the wind density, which is assumed to be 1.225kg/m^3 at sea level at 15°C, and V is the speed of wind.

$$q_s = \frac{\rho V^2}{2} \tag{1.1}$$

Using Equation 1.1 and the minimum pressure calculated from the differential pressure datasheet, the minimum velocity it can record is 16m/s, meaning it does not satisfy the design criteria outlined in [9].

Sensirion's ASP1400 differential pressure sensor [11] is capable of measuring 0.002Pa to 100Pa with a resolution 0.001Pa, allowing the device to record airspeeds below 5m/s with high accuracy. The sampling time can range from 0.78Hz to 7Hz, making the device too slow to satisfy the design criteria.

For small UAVs, keeping external devices lightweight and low power is vital to maintain a reasonable flight time. The ultrasonic airspeed sensor design is compared to ClimaTec's CYG-81000 ultrasonic anemometer [12], which is capable of measuring airspeeds of 0m/s to 40m/s with a resolution of 0.01m/s at an output rate of 4Hz to 32Hz. This comes at the cost of requiring a DC supply voltage of 24V, and weighting 1.7kg. The aircraft used in [9] weights 1.06kg, which shows that the ultrasonic anemometer is not suitable for their use case, as the anemometer weighs significantly more than the aircraft itself. The ultrasonic airspeed sensor requires a DC supply voltage of 3.3V, and weights 0.171kg, showing that the ultrasonic airspeed sensor provides a suitable middle ground for obtaining accurate airspeed measurements, while maintaining a lightweight design suitable for small UAVs.

Design methodologies for ultrasonic airspeed sensors can be seen in [13, 14]. These designs focus on creating an ultrasonic airspeed sensor with at least two axes of wind velocity information. This design is necessary for quadcopter UAVs, as these devices are capable of forward/backward flight and left/right flight. This thesis is focused

on designing an ultrasonic airspeed sensor for fixed-wing UAV, which is capable of forward flight only. Data relating to wind velocity coming from the front of the fixed-wing UAV is necessary, while other axes can be disregarded. This requires a single ultrasonic transceiver pair, which will reduce the power consumption and weight of the design compared to the design presented in [9]. A prototype one-axis ultrasonic airspeed sensor design is presented in [15]. The design records airspeed data using one ultrasonic transmitter and two ultrasonic receivers, using the Doppler beam swinging technique. An analog signal processing chain was developed to extract the transmitted ultrasonic signal from a noisy environment, through a mixture of low pass filters and band pass filters centred at 38kHz. Figure 1.1 compares the performance of an ultrasonic anemometer to the performance of the one-axis ultrasonic airspeed sensor.

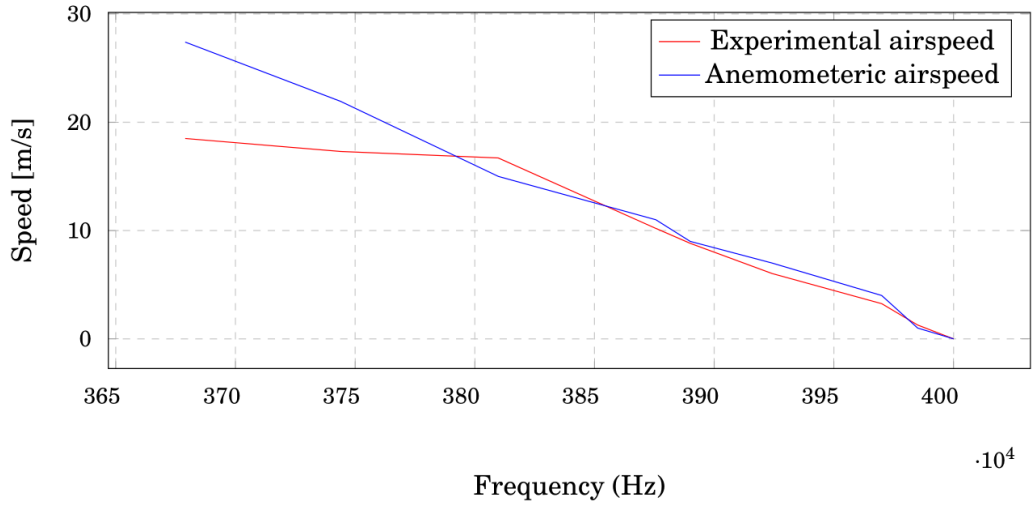

Figure 1.1: Airspeed measurements from ultrasonic airspeed sensor and ultrasonic anemometer from [15].

The device is capable of recording airspeeds from 0m/s to 17m/s, where the results begin to deteriorate after 17m/s. No information is available on the accuracy or precision of the prototype ultrasonic airspeed sensor data. This information is vital for low speed flight, as the target fixed-wing drone has a stall speed from 10m/s to 12m/s.

1.4 Thesis outline

The purpose of this thesis is to develop an ultrasonic airspeed sensor for a lightweight fixed-wing drone. Chapter 2 establishes the fundamentals of Pitot-static systems and ultrasonic systems, and their usage as air flow measurement devices. Environmental effects that can alter the speed of sound are discussed, along with a short section on signal conditioning and digitisation. Chapter 3 outlines methodology and tools used to develop the ultrasonic airspeed sensor. Chapter 4 focuses on the pre-design stage, where an ultrasonic distance sensor is reverse engineered, and how the design can be applied to an ultrasonic airspeed sensor design. Chapter 5 delves into the

full design of the ultrasonic airspeed sensor, including defining the hardware and software used to create the sensor. Chapter 6 presents the results of the design, and verifies the functionality of the ultrasonic airspeed sensor. This chapter will highlight specific design requirements, and verify if these requirements have been achieved. Chapter 7 provides a discussion on the ultrasonic airspeed sensor results, along detailing methods for improving upon the current ultrasonic airspeed sensor. This includes alternative design choices, flight controller integration and factors to consider when calibrating the system. A reflection on the project planning and ethical considerations of the project is discussed in this chapter. Chapter 8 will conclude the report.

2
Technical background

This chapter provides context to the technical principles used to design the prototype ultrasonic sensor. This chapter begins with a discussion on commercially available products for measuring airspeed and wind speeds, and how their functional principles can be merged to produce an ultrasonic airspeed sensor. The theory of signal processing is discussed, where different methods of signal filtering are reviewed.

2.1 Uncrewed aerial vehicles (UAV)

Uncrewed aerial vehicles (UAV), or drones, refer to any aerial vehicle which does not carry a human operator, but can be controlled remotely or through an autonomous system. This definition ranges from radio controlled model aircraft to modern autonomous quadcopter drones. The applications of UAVs is diverse, but UAVs are most commonly associated with expensive miliary aircraft or small consumer drones [16]. Commercial and research applications for drones have risen in recent years, including emergency services, filming, photography, infrastructure inspections and mapping.

2.2 Pitot-static systems

A standard airspeed measurement device for commercial aircraft are Pitot-static systems. These devices function as a differential pressure flow meter, calculating the difference in recorded total pressure and recorded static pressure to obtain the dynamic pressure.

2.2.1 Implementation

The device has a tube which protrudes from the body of the aircraft. This is the Pitot tube port, which measures the total pressure developed by the forward speed of an aircraft [17]. The static pressure is sensed by orifices in the side of another type of tube, called a static-pressure tube, or by a set of holes in the side of the aircraft body, called static ports or fuselage vents. The Pitot tube and static-pressure port come as two separate units, or combined into one unit. By measuring the total pressure P_t and static pressure p, the dynamic pressure q_c can be determined by Equation 2.1.

$$P_t = p + q_c \tag{2.1}$$

In incompressible flow, the pressure developed by the forward motion of a body is called the dynamic pressure, q_c, which is related to the airspeed [17]. This relationship is shown in Equation 2.2, where ρ is the density of air, and V is the speed of the aircraft relative to the air.

$$q_c = \frac{\rho(V^2)}{2} \tag{2.2}$$

Equation 2.2 is used to determine the indicated airspeed of the aircraft. Using further signal processing, such as sensor fusion and position correction, the true airspeed can be determined. It should be noted that air is compressible, and when airspeed is measured with a Pitot-static tube, the air is compressed as it is brought to a stop in the pitot tube [17]. For low subsonic conditions, the compressibility is ignored. Different equations are required for supersonic flight, however these equations are outside of the thesis scope.

2.2.2 Measurement error

The placement of airspeed measurement ports is crucial to obtaining accurate airspeed results. The purpose of the Pitot-static system is to obtain the air pressure readings within the 'freestream', which is an area where the airflow is undisturbed. Disturbances in airflow are caused by engine emissions or air reflected by the aircraft body entering the measurement ports. This type of error is defined as 'Position Error' [18], and can effect readings obtained from the static port or Pitot tube. The effect of this error is more likely to occur on static pressure ports, as the static pressure local value can vary greatly depending on the position of the port along the drone body. The static pressure field varies with changes in the aircraft configuration, angle of attack, airspeed, and angle of travel relative to the wind. This error is present within all forms of airspeed measurement equipment, as any physical object which interacts with the freestream will disturb the airflow. The significance of the error will depend on its placement relative to the aircraft body, and size of the airspeed sensor. This error needs to be accounted for to determine the calibrated airspeed.

A variety of mechanical sources of error can exist within the Pitot-static system. The pressure at an instrument can be different from the pressure at the pressure source because of a time lag in the transmission of pressure. The pressure at the instrument can also differ from that at the pressure source when there is a leak in the pressure system [17]. Blockages within the tube system can either lead to complete instrumental failure if air cannot enter the tubes, or produce inaccurate results when air is blocked within the Pitot-static system. Trapped air within the Pitot-static system is more difficult to notice, as a blockage will present itself as a gradual loss of pressure and airspeed [19]. This can cause pilots to over compensate for the apparent decrease in airspeed, leading to a loss of control and potential accidents.

Harsh weather environments can cause water to enter the Pitot-static system, leading to inaccurate results. This is prevented by heating the tubing system, causing the water to evaporate. This proves useful when the trapped water is clean, however residue from salt water can build up within the system if flying the drone

near the sea. This will cause inaccurate results and mechanical deterioration to the device.

Measurement of airspeed at low velocities is difficult for a Pitot tube to record, as the difference in total pressure to static pressure is significantly reduced. This uncertainty is elevated even further when we consider Equation 2.2, as the velocity has a non-linear relationship with the total and static pressures. This causes the resolution of the system to decrease as the aircraft velocity decreases, which makes it difficult to rely on Pitot-static systems for automated landing and take-off procedures, or operating at speeds close to stall speeds.

2.3 Ultrasonic sensors

Ultrasonic sensors use sound waves above the 20kHz range to detect objects within a certain proximity, without making physical contact to the object [20]. The ultrasonic sensor is a piezoelectric transducer. Ultrasonic transmitter is able to convert an electrical signal into a mechanical vibration, and ultrasonic receivers can convert a mechanical vibration into an electrical signal. Microphones and speakers can be compared to ultrasonic receivers and transmitters, however ultrasonic sensors are created to operate within a significantly smaller frequency range. This prevents the ultrasonic receiver from picking up noise within the environment, ensuring the only signal it receives is the transmitted ultrasonic signal.

Ultrasonic systems can be monostatic or bistatic, where bistatic systems use separate piezoelectric transducers for transmission and receiving, while monostatic systems use one piezoelectric transducer for transmission and receiving [20].

The non-contact aspect of the ultrasonic sensors makes them suitable for industrial automation, such as for object detection or collision avoidance applications. Ultrasonic sensors are often used for instrumentation applications, such as for ultrasonic anemometers, tide gauges, and non-intrusive gas flow detection systems.

2.4 Methods of utilising ultrasonic sensors

The main purpose of ultrasonic sensors is to measure the transit time between an ultrasonic transmitter and receiver. The system structure and distance calculating algorithm can change depending on the application. For automation object detection applications, the most common setup consists of the ultrasonic transmitter and receiver being placed together on the mobile robot. These devices will use a Time of Flight algorithm, where an ultrasonic signal will be transmitted, and receive an echo from local objects. This allows for the velocity of the ultrasonic signal to act as a constant, where the transmission time will be detected by the ultrasonic system. Using these two values, the distance of the ultrasonic system to a local object can be determined.

For transit time ultrasonic flow meters and ultrasonic anemometers, the transmission distance remains constant. The ultrasonic signal will pass through a varying medium, which causes the speed of sound to change. Transmission medium properties that can alter the speed of sound include temperature, pressure variations and

chemical composition of the medium. The ultrasonic signal can be superposed by other velocities within the transmission medium, such as liquid or gas flow, causing the transmission time to increase or decrease depending on the transmission angle relative to the flow.

The Doppler effect applies to all wave energy, including sound. The Doppler effect is used for Doppler ultrasonic flow meters, where the device will transmit an ultrasonic beam into a stream flowing through a pipe [21]. This method is typically used for measuring the flow of dirty fluids, such as mining slurries, raw wastewater and sludge. The presence of acoustical discontinuities, such as solids or air bubbles, are essential for the operation of Doppler flow meters.

Variations of each system setup and computational method exist, such as Doppler Velocity Loggers (DVL) for underwater vehicle velocity measurements, or ultrasonic motion sensors for home security. This shows that the range of applications for ultrasonic sensors is diverse. Considering the variety of methods of utilising ultrasonic sensors, each method should be evaluated with respect to airspeed measurements.

A typical block diagram for an ultrasonic system can be seen in Figure 2.1. The system consists of an analog front end for driving the ultrasonic transmitter, along with an analog signal conditioning architecture before digitising the ultrasonic signal for further processing.

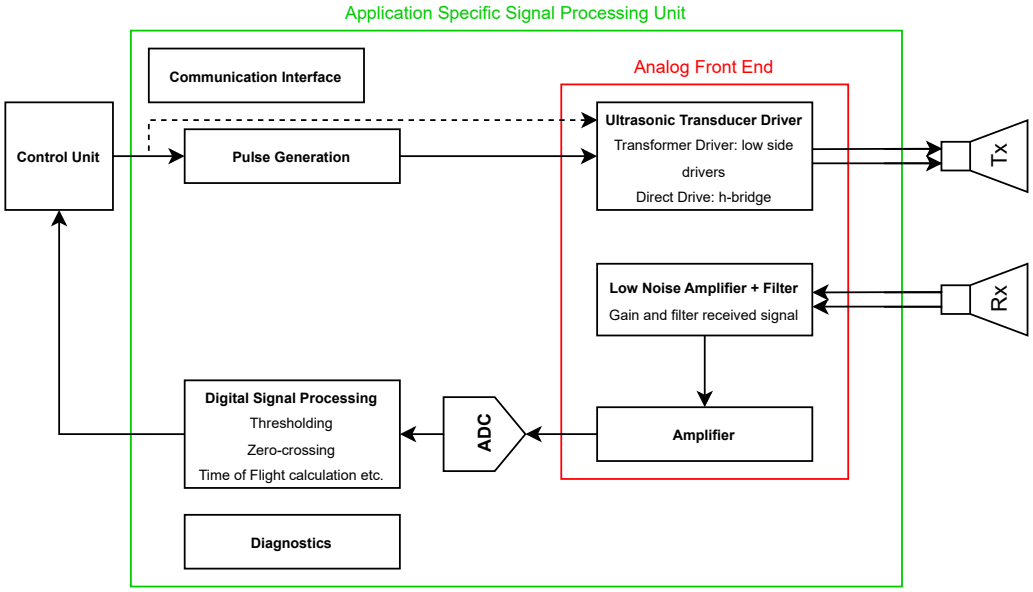

Figure 2.1: Ultrasonic system level block diagram [20].

2.4.1 Time of flight (ToF) ultrasonic sensors

Ultrasonic distance sensors operate by sending out a series of ultrasonic pulses within its field of view, and measuring the time it takes for the sound wave to reflect off a target and return to the ultrasonic receiver [20]. Equation 2.3 is used to determine the distance D of the ultrasonic sensor from the target. t equals the time taken from initial transmission to receive the signal back to the transmitter. c equals the

speed of sound, which at room temperature, is assumed to be 343m/s. Since the ultrasonic signal needs to travel to the target and back to the receiver, Equation 2.3 is divided by two.

$$D = \frac{t \cdot c}{2} \tag{2.3}$$

Considering Equation 2.3 only contains two variables, of which one is usually assumed to be a constant, the ultrasonic sensor can obtain precise measurements within a controlled environment, and can operate within a real-time environment with minimal computational power required.

These devices are the most commonly known ultrasonic sensors, as their popularity have grown within the hobbyist communities.

2.4.2 Transit time ultrasonic sensors

Transit time ultrasonic sensors use a similar principle to Time of Flight ultrasonic sensors. Both methods use Equation 2.3, however for transit time calculations, the distance is static, and the transmission time will change as the transmission medium changes. The speed of sound is dependent on temperature, humidity, air pressure [20], and can be superposed by external velocities. For transit time ultrasonic flow meters, the ultrasonic signal will need to pass through a pipe of a known diameter and material, and pass through a known liquid or gas where the flow velocity is unknown.

The characteristics that alter the transit time can be considered as one of two categories: scalars or vectors. Scalar factors will consider temperature, pressure or chemical composition, where their effects on the transmission medium are irrespective of transmission direction. Vector factors will consider the flow of a gas or liquid, which will contain a magnitude and direction. These vector factors will change the transit time depending on their direction relative to the ultrasonic transmission direction. By transmitting an ultrasonic signal upstream and downstream, the system can differentiate the impact of scalar and vector transmission medium properties on transit time through the superposition principle. This method can distinguish the sum of static transmission medium characteristics and the sum of vector transmission medium characteristics. If the effects of individual transmission medium characteristics need to be determined, additional sensors are necessary.

2.4.3 Doppler ultrasonic sensors

Doppler ultrasonic flow meters function on the Doppler effect principle, where the frequency of a sound wave received by an observer is dependent upon the motion of the source or observer in relation to the source of the sound. For Doppler ultrasonic flow meters, the Doppler effect is used to determine the velocity of discontinuities within a pipe, as the transmitter and receiver are stationary. Equation 2.4 shows how a Doppler ultrasonic flow meter determines the flow velocity V of a fluid within a pipe [21]. f_0 is the transmission frequency, f_1 is the reflected frequency, C_t is the velocity of sound inside the transducer, and a is the angle of the transmitter and receiver with respect to the pipe axis. Since a Doppler ultrasonic flow meter

is installed within a controlled environment, $C_t/2f_0\cos(a)$ is considered to be a constant.

$$V = \frac{(f_0 - f_1)C_t}{2f_0\cos(a)} \tag{2.4}$$

2.5 Ultrasonic anemometers

The most similar current technology to replicate an ultrasonic airspeed sensor is an ultrasonic anemometer. Ultrasonic anemometers are wind recording devices, which are replacing the 'spinning cups' or propeller mechanical wind measurement devices within the field of meteorology. Ultrasonic anemometers have proven to be more accurate and precise than mechanical anemometers, along with being more robust due to containing no moving parts. Ultrasonic anemometers require two ultrasonic sensors to record data within one dimension, with a minimum of six ultrasonic sensors required to obtain three dimensional wind data.

The usage of ultrasonic anemometers as a replacement for Pitot tubes is rare, but has proven useful in one case. The Hamadori is an uncrewed fixed-wing seaplane developed by Space Entertainment Laboratory, used primarily for ocean data collection [22]. The Hamadori is capable of landing and taking off from the ocean surface, meaning that the Hamadori frequently comes in contact with splashing saltwater. This leaves the Pitot tube system prone to blockages due to saltwater entering the ports, which will lead to inaccurate airspeed measurements. Heating the Pitot tube can extend the operation lifespan of the system when these problems are encountered, however the evaporated saltwater will leave salt crystals and minerals within the Pitot tube system. In an attempt to fix this problem, Space Entertainment Laboratory collaborated with FT Technologies to integrate an FT205 wind sensor [23] onto their fixed-wing drone as an alternative to Pitot tubes. This has proven to be more robust and reliable than their previous Pitot tube system, especially when the Hamadori remains in contact with the ocean surface for long periods of time.

An example of a one-dimensional (1D) ultrasonic anemometer is the Ultrasonic Anemometer 1D developed by Thies Clima [24]. This device has a measuring range of 0m/s to 75m/s, with a resolution of 0.1m/s and an accuracy of $\pm$2%rms at wind speeds above 5m/s. 1D anemometers are suited towards applications where the direction of wind flow is known, such as within tunnels and tubes.

2.5.1 Working principle

Ultrasonic anemometers use a transit time ultrasonic system to determine wind velocity. These devices use ultrasonic transceivers, which are capable of receiving and transmitting ultrasonic signals depending on their selected mode. The most common form of ultrasonic anemometer consists of four ultrasonic transceivers, where two transceivers are required for measurements within one axis.

The distance between each transceiver pair is known, meaning the device is used to calculate the changing speed of sound. The speed of sound will be altered by the transmission medium and superposition of wind velocity. Ultrasonic anemometers

are capable of differentiating the effects of both characteristics on the speed of sound. Wind velocity will contain a directional component, while all other transmission medium characteristics, such as temperature, pressure and humidity, will not contain a directional component. If a signal is transmitted in a direction which is non-perpendicular to the wind direction, each transceiver will produce a different result. The 1D Anemometer uses two ultrasonic transceivers, where the propagation time of sound is measured upstream and downstream from the wind velocity. This will produce two different results, as propagating a signal upstream will reduce the speed of propagation, and propagating a signal downstream will increase the speed of propagation. The average of both results determines the speed of sound in the environment without the influence of wind, which is used to compute the wind velocity.

Figure 2.2 shows the working direction of the 1D Anemometer [24]. The device is placed within a tunnel or tube, where the walls of the tunnel can be seen in the top and bottom of Figure 2.2, implying that the wind is mostly present within one axis.

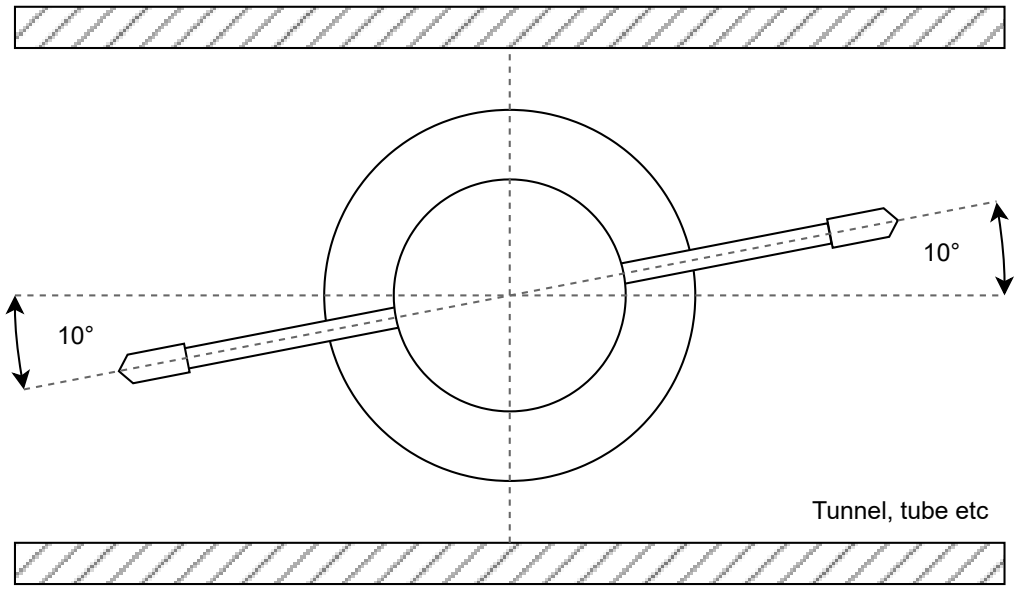

Figure 2.2: Thies Clima 1D Anemometer working direction [24].

The system is placed ±10° relative to the expected direction of wind. For the Ultrasonic 1D anemometer, only the Y-component of the wind velocity vector is analysed, meaning the X-component is not acquired. If an angle of attack is predicted as ±10°, the recorded value can be corrected by dividing the recorded velocity by a factor of cos(10°) or 1.5%. It is uncertain if the device corrects the velocity value with this factor.

2.6 Transmission medium properties

Transmission properties, and the speed of sound, change across different mediums. An ultrasonic sensor is optimised for sound wave propagation through gas, liquids or solids, but rarely for more than one type of transmission medium [20]. The speed of sound is 343m/s when propagating through dry air at 20°C. The velocity is influenced by external environmental parameters, such as temperature, relative humidity, in-band ambient noise, change in pressure, and change in air mixture. The influence of humidity, temperature, pressure and CO_2 concentration have all been considered in [26], with humidity and temperature influencing the speed of sound the most. The speed of sound can range from 325m/s to 355m/s when considering temperature ranges of -10°C to 30°C, and a relative humidity of 0% to 100%. Factors such as pressure and CO_2 concentration do influence the speed of sound, however their influence is negligible [26]. This means that the measuring range of the ultrasonic anemometer is influenced by two main factors: the airspeed velocity range of interest, and the operating conditions of the device.

2.7 Signal conditioning

Ultrasonic receivers convert mechanical vibrations into electrical signals, which must be processed to extract relevant information from the electrical signal. A designer has a wide range of techniques available to them for processing a signal, where the combination of processes are unique to the received electrical signal and required data for analysis. Two domains of signal processing exist, analog and digital signal processing. Analog signals are continuous and have an infinite resolution, while digital signals are sampled signals represented in binary format. Every signal processing chain that consists of a physical signal that needs to be interpreted by a computer will contain a mixture of analog and digital components. The quantity and complexity of analog and digital components will depend on the quality of the received signal and the desired information from the signal. The analog signal needs to be in a condition that is suitable for digitising, which means that filtering systems must be employed to remove unwanted features within the signal. The amplitude of the signal must be large enough to trigger the quantisation levels of the analog to digital converter, or to trigger a comparator.

2.8 Filters

Filtering systems are used to remove unwanted features within a signal. These filters are created by understanding the frequency of the relevant signal, and developing a filtering system which is capable of removing all other signal features. Two categories of filters exist: analog and digital filters. Analog filters use physical hardware, which provides the advantage of faster signal processing, higher amplitude dynamic range, and higher frequency dynamic range. This comes at the cost of precision, such as introducing larger passband ripple, lower roll-off rate, and a decreased stopband attenuation [29]. Digital filters are better suited for designs which require

high precision, as digital filters do not require component matching. The extent that each filtering category is used is dependent on the application, with the main considerations being delay and filtering precision.

2.8.1 Analog filters

Analog filters can be categorised as passive or active filters. Passive filters are constructed using resistors, inductors and capacitors. These devices do not require an external power source, meaning that the design is simpler and less expensive, however this means that it cannot produce a power gain to the signal. With the usage of inductors, the passive filters are suitable for high current, high frequency applications, at the cost of being bulkier.

Active filters use operational amplifiers or transistors in combination with resistors and capacitors. Operational amplifiers require a constant power source to operate, which allows for the device to increase the power of the filtered signal. Active filters do not require inductors, which can reduce the size of the filtering system. Designing filters with active components is more expensive and complicated, but allows for greater control over the filter characteristics; therefore the differences of passive or active filters must be considered with respect to the application.

2.8.2 Digital filters

There are two basic types of digital filters: finite impulse response (FIR) filters and infinite impulse response (IIR) filters. FIR filters use a finite number of samples to produce an impulse response output that settles to a steady-state value after a finite duration [30]. The filter uses previous and current input values, without using previous output values to produce an output, making it non-recursive and inherently stable. These filters introduce a constant delay across frequencies to the input signal. Figure 2.3 shows a block diagram for a FIR filter, where the input is represented by $x[n]$, and z^{-1} represents a finite number of previous input samples. These samples are multiplied by coefficient values b, and summed together to create the output $y[n]$. The coefficient values are an array that represents the filtering type and its characteristics. More coefficient values or taps will produce a higher quality filtering system, at the cost of increasing delay and computational power.

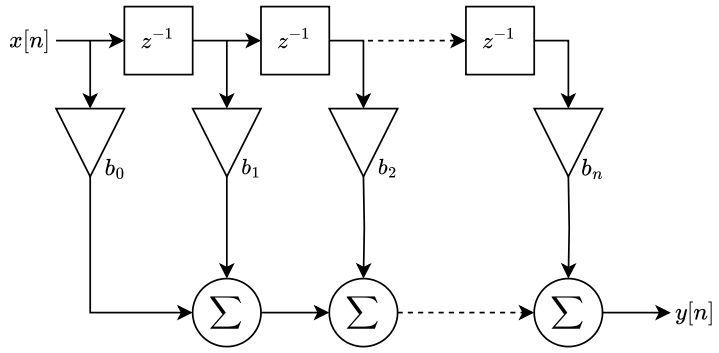

Figure 2.3: FIR filter block diagram [30].

IIR filters are recursive filters that depend on both the filter input values and the filter output values, creating a feedback loop [30]. This can cause IIR filters to become unstable if they are not carefully designed, since the IIR filter does not settle to a steady-state value. IIR filters are generally faster [29] and require less memory space [31] than a comparable FIR filter. Figure 2.4 shows a block diagram for an IIR filter, which has a similar operation to the FIR filter, however previous outputs of $y[n]$ are multiplied by coefficient values $-a$, and summed with previous inputs of $x[n]$ that have been multiplied by their respective coefficient values b.

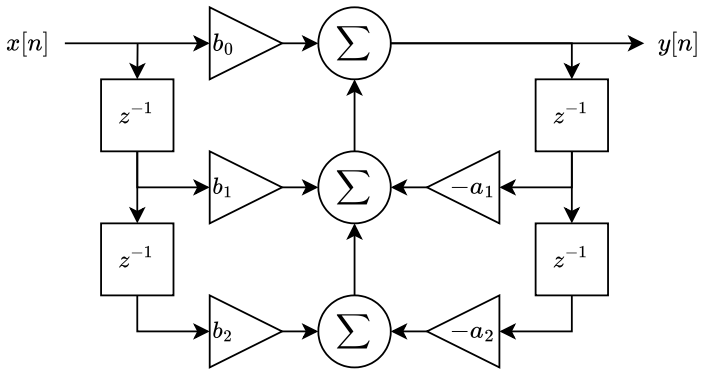

Figure 2.4: IIR filter block diagram [30].

Kalman filters function as a mean squared error minimiser [32], which has been applied to a wide range of tracking and navigation problems. A Kalman filter shares similarities to an optimal FIR filter in the mean squared sense, however the Kalman filter skips the need to determine the impulse response of the filter by considering the data in state-space. Figure 2.5 shows the Kalman filter recursive algorithm, which uses previous data estimates and the current data input to create predictions of future data within state-space.

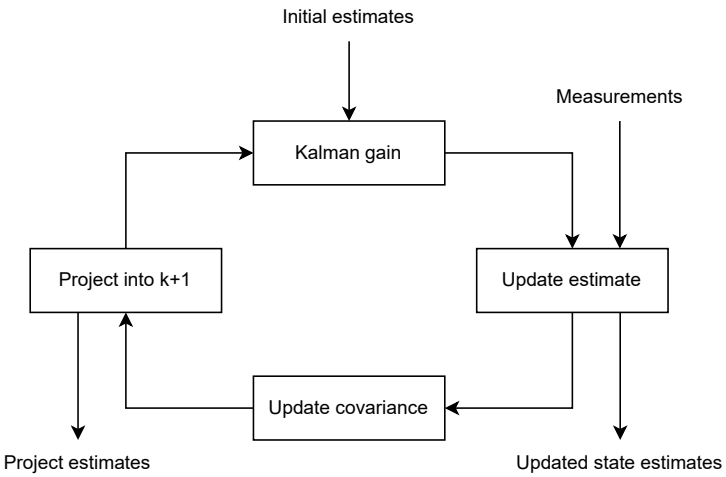

Figure 2.5: Kalman filter recursive algorithm [32].

3
Approach

The development process of the ultrasonic airspeed sensor contains several key steps. An initial study into the working concepts of Pitot-static systems is performed to gain an understanding of their working principle and performance characteristics. This study is used to establish the minimum performance criteria for the ultrasonic airspeed sensor, and justify the development of the ultrasonic airspeed sensor with respect to the Pitot-static system sources of error.

A survey of ultrasonic products is conducted to gain an understanding of conceptual and commercially available ultrasonic devices, including ultrasonic distance sensors, flow meters, anemometers and prototype airspeed sensors. Through this process, multiple methods of implementing ultrasonic technologies are evaluated to determine the most suitable method for developing an ultrasonic airspeed sensor for lightweight fixed-wing drones.

Two ultrasonic products are selected as inspiration for the ultrasonic airspeed sensor: the HC-SR04 ultrasonic distance sensor, and the 1-D ultrasonic anemometer. The hardware of the HC-SR04 is analysed to obtain an understanding of low-cost ultrasonic signal processing techniques, while the 1-D ultrasonic anemometer is analysed to determine methods of high-accuracy wind measurements.

3.1 Hardware design

The hardware design is inspired by low-cost ultrasonic distance sensors. These types of devices have become increasingly popular within hobbyist communities for automation and instrumentation projects. Their low cost and low power consumption makes them an ideal starting point for developing the analog signal processing chain for the ultrasonic airspeed sensor, along with selecting suitable components for circuit construction.

3.1.1 Analog circuit development

The received ultrasonic signal must undergo signal processing before the signal can be analysed. The bandwidth of the signal should be limited to frequencies of interest, to ensure that the signal is not influenced by external distortions. Restricting the bandwidth of the signal ensures that the signal can be sufficiently sampled by an analog to digital converter for further signal processing. To ensure that the full resolution span of an analog to digital converter is used, the ultrasonic signal should be unipolar, and the peak-to-peak voltage must match the voltage reference. This

requires the usage of active signal processing components to amplify the received ultrasonic signal, and generate the necessary offsets to turn a bipolar signal to a unipolar signal.

A control circuit must be developed to obtain upstream and downstream velocity recordings. Both values are required to obtain wind velocity measurements, therefore the ultrasonic transceiver roles will continuously change. The driving ultrasonic signal and received ultrasonic signal are connected to the same ultrasonic transceiver pin, therefore a control circuit is required to ensure that the transmitting ultrasonic transceiver is isolated from the signal processing circuit. This will prevent the driving signal from distorting the received signal.

The analog circuit is developed using LTspice [33], an analog electronic circuit simulator developed by Analog Devices. LTspice provides a library of simulation models to represent real passive and active components. SPICE models are often provided by component suppliers, and can be imported to LTspice if the models are not present in the default library.

To assist with developing the analog filter, Analog Devices provides an Analog Filter Wizard [34] used for generating analog low pass, high pass and bandpass filters. The Analog Filter Wizard allows for the user to select the filter characteristics and generates a variety of schematics based off the design requirements. Each schematic comes with a range of components recommended for circuit construction, along with describing why such components were selected.

The analog filtering system is verified using LTspice, and the MATLAB Control System Toolbox [35]. These are used to generate filter frequency response diagrams in magnitude and phase. An ideal filter is generated, and depending on the components available and their tolerances, a more realistic filter response is analysed. This step is crucial to ensure that the filtering system is capable of removing noise within the received ultrasonic signal, and limiting the bandwidth of the signal to provide a platform for ADC conversions.

3.1.2 Ultrasonic airspeed sensor testing rig

A mechanical testing rig is developed to ensure that the distances between the ultrasonic transceivers is constant, and to provide support to the device during wind testing. The majority of the airspeed sensor hardware will be stored inside the drone itself, however the transceivers will protrude from the drone body to allow for airspeed measurements. This will be designed using Autodesk Fusion [36] and imported to PrusaSlicer 2.9.2 [37] to allow for 3D printing. A simple prototype is necessary, as the testing rig is not used when integrating the airspeed sensor to the drone.

3.2 Software design

The software has three main functions for the ultrasonic airspeed sensor: controlling the ultrasonic sensors, recording the time from PWM signal generation to receiving the ultrasonic signal, and calculating the wind speed velocity through the upstream

and downstream values. The software design is implemented on an ESP32 microcontroller, using the Arduino IDE as a coding platform. The ESP32 microcontroller was selected to provide a simple, but powerful platform for software development. The Arduino IDE [38] supports the usage of a simplified version of C++, which contains specific libraries for the selected target microcontroller. The ESP32 has a maximum clock speed of 240MHz, making the device suitable for real-time digital signal processing purposes. Generating real-time wind speed data is crucial for autonomous flight, and ensuring that the fixed-wing drone does not stall due to lagging wind speed data.

3.2.1 Wind speed calculations

Wind speed calculations begin with obtaining the transmission time of upstream and downstream ultrasonic transmissions. The distance between ultrasonic transceivers is constant, meaning any difference in transmission time is caused by a changing speed of sound. This is used to determine the speed of sound when transmitting an ultrasonic upstream and downstream. The median value of upstream and downstream transmission is the speed of sound without the influence of wind, and the difference in the median to upstream or downstream velocities relates to the wind speed. This value is used to determine the indicated airspeed.

3.2.2 Control sequence

The control sequence ensures that the correct ultrasonic transceiver is in transmission or reception mode, and ensuring that the correct data has sufficient time for processing. The following factors need to be considered for the timing of this control sequence:

- The transmission driving signal will consist of a 40kHz signal, and all the odd harmonics of the 40kHz signal required to generate a PWM. If the timing is incorrect or the received and driving signal are not isolated, there is a risk of the PWM signal interfering with the received ultrasonic signal. While filtering the ultrasonic signal will prevent the appearance of those odd harmonics, the 40kHz PWM signal cannot be separated from the received ultrasonic signal. Therefore, the transition time needs to be long enough to ensure that the receiving ultrasonic transceiver is oscillating high enough to become the dominant signal in the system.
- The transition time needs to be long enough to allow for the ringing-decay effect of the transmitting ultrasonic transceiver to dissipate, as the system may interpret the ringing as a received ultrasonic signal.
- The transition time needs to be long enough to allow for data processing, ensuring that data registers are not corrupted by new data entering the system too quickly.
- The transition time between changing states must be kept low, to ensure that real-time upstream and downstream data can be collected. Preventing the system from transitioning for too long will cause the data to inaccurately reflect the true airspeed.

3.2.3 Component communication protocol

The ultrasonic airspeed sensor is intended for integration with open-source flight controlling software. An example software is ArduPilot, which supports a wide variety of communication protocols for sensor integration, including I2C, SPI, UART and CANBUS [44].

For the ultrasonic airspeed sensor, the SPI interface is selected for communications between components. The SPI interface is known for having high transmission rates [45], which ensures that data transmission bottlenecks are not caused by the communication interface. This method allows for full duplex communication, which can open up possibilities for more complex calibration sequences and altering the airspeed sensor variables without changing internal code.

The usage of digital communication protocols are required for interfacing with analog to digital converters, therefore an ADC with a similar communication protocol is recommended. This will ensure that a unified communication protocol is present within the entire design. In the case that an ADC is not used within the system, an SPI interface is still necessary for communications between the ultrasonic airspeed sensor and the flight controller.

One of the limiting factors of SPI is the communication distance, which is limited to 10m without the use of repeaters [46]. For the fixed-wing drone, the communication distances are substantially lower than this, ensuring that attenuation caused by increased line resistance will not distort transmission data.

3.3 Calibration sequence

The calibration process will investigate the effects of sensor position and size on freestream disturbances. The purpose of the ultrasonic airspeed sensor is to record freestream data, however any physical object that interacts with the freestream will cause its own disturbances. This problem is present within all airspeed sensors, requiring a calibration process to compensate for these errors. Without this process, the ultrasonic airspeed sensor is limited to providing indicated airspeed readings, where calibrated airspeed readings are required to obtain equivalent and true airspeed readings. The accuracy of airspeed readings are particularly important for autonomous flight at close to stalling speeds, therefore any method to improve the accuracy is valuable.

3.3.1 Data processing

The Arduino IDE is capable of showing the user the results as they arrive, however no logging capabilities are built into the IDE. Data is recorded through the ESP32 serial interface using PuTTY [47], a serial console application. This data is analysed using MATLAB, where airspeed velocity graphs are produced.

4

Technical pre-design

To begin designing the ultrasonic airspeed sensor, an analysis of commercially available ultrasonic sensors is required. This involves focusing on two categories of ultrasonic sensors: ultrasonic anemometers and ultrasonic distance sensors.

Ultrasonic anemometers are the closest equivalent technology to the ultrasonic airspeed sensor, so the design will be based of their working principles. These devices consist of ultrasonic transceiver pairs, that are placed a predetermined distance from each other. The ultrasonic transceiver pairs transmit an ultrasonic signal back and forth between each other, to generate upstream and downstream time recordings within one axis of interest. The median value of upstream and downstream time recordings will correlate to the speed of sound due to environmental influences, such as temperature and humidity. The difference in the median value to upstream or downstream time values will indicate the influence of wind on the speed of sound. Using this value and the transceivers distance of separation, the velocity of wind can be determined.

Ultrasonic anemometers can be expensive, heavy, and consume a large amount of power. The 1D ultrasonic anemometer mentioned in Section 2.5 requires a minimum power supply of $8V_{DC}$ or $12V_{AC}$ to operate, with an additional 24V, 40W power required for its heating components [24]. For lightweight drone applications, this will greatly reduce the flight time of the drone. The ultrasonic anemometer weights 2.5kg, making the device unsuitable for a drone which has a maximum take-off weight of 1kg.

A lightweight, low-cost alternative is ultrasonic distance sensors. The hardware architecture will be based off commercially available ultrasonic distance sensors, such as the HC-SR04. This device requires an operating power of 5V, 15mA, and weights 8.5g, making it suitable for lightweight drone applications. The hardware of the HC-SR04 will be reverse engineered, and used as an inspiration for developing hardware for the ultrasonic airspeed sensor. Combining the software of an ultrasonic anemometer and hardware of an ultrasonic distance sensor, an ultrasonic airspeed sensor can be developed to record the indicated airspeed.

A calibration process is required to obtain calibrated airspeed measurements. The main purpose of the ultrasonic airspeed sensor is to measure the velocity of wind when it has not been disturbed by the drone body. Disturbances caused by the ultrasonic sensor itself are unavoidable, and must be accounted for to obtain the calibrated airspeed.

4.1 Hardware design

The initial hardware design phase begins with reverse engineering a commercially available ultrasonic distance sensor. This is to understand how an ultrasonic transmitter and receiver system functions, specifically the control functions and signal processing system. A HC-SR04 ultrasonic distance sensor was selected for this purpose, as the HC-SR04 is a low-cost device that is commonly used for Arduino based hobby projects. A wide range of community created documentation is available for this device, along with documentation relating to improving the onboard PCB for more accurate distance measurements.

Once this has been reverse engineered, ultrasonic transceivers were selected for this project, which differ from the HC-SR04 ultrasonic transducers. The HC-SR04 is a bistatic system, meaning it has separate piezoelectric components for receiving and transmitting an ultrasonic signal. The selected ultrasonic transceivers are monostatic, meaning one piezoelectric is capable of transmitting and receiving a signal. This means the HC-SR04 architecture cannot accomodate for the ultrasonic transceivers without modifications. The ultrasonic transceivers are tested using oscilloscopes and waveform generators, to get an understanding of how these devices transmit and receive signals. A control and signal processing system is developed for the ultrasonic transceivers, based off the HC-SR04 design.

The ultrasonic transceiver circuit consists of two main components: transmission and reception controls, and the signal processing board. The transmission and reception controls are used to select which transceiver is connected to the ultrasonic driving circuit, and which transceiver is connected to the signal processing board. To compute wind velocity data, the transceiver system requires upstream and downstream transmission time values, therefore their roles within the system will constantly change. The purpose of the signal processing board is to modify the received ultrasonic signal, so that it is suitable for analog to digital conversion.

4.2 HC-SR04

The HC-SR04 is an ultrasonic distance sensor, which is popular for Arduino based object detection projects for hobbyists. This device determines its distance from a target through Time of Flight calculations, where it has a ranging distance of 2cm to 400cm, with a resolution of 0.3cm [39]. Figure 4.1 shows the HC-SR04 sensor used within this thesis.

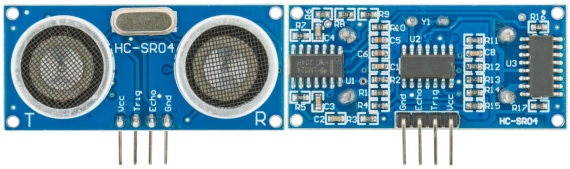

Figure 4.1: HC-SR04 sensor, front and back.

4.2.1 Operation

Multiple variations of this design exist, as the device design has been repurposed by different companies, where their iterations do not contain version numbers to distinguish themselves from others. This has made it difficult to find documentation relating to the exact components that exist within the device, however all HC-SR04 devices have the same functional operation. This thesis will analyse the HC-SR04 available from [39]. The HC-SR04 sensor contains four pins: 5V input voltage, ground, a trigger input pin and an echo output pin. The trigger pin is used to activate the ultrasonic transmitter sensor by transmitting a TTL signal for 10μs from an Arduino to the HC-SR04 sensor. This causes the HC-SR04 circuit to transmit eight 40kHz pulses to the ultrasonic transmitter, producing a 40kHz ultrasonic signal. After a short delay, the Echo pin will output a TTL signal, and stay high until the system has received the ultrasonic signal again. The Echo pin delay is necessary to ensure that the ultrasonic receiver is receiving the ultrasonic echo, and not the original transmitted ultrasonic signal. The TTL signal width represents the total transmission time t, which is used to calculate the sensor distance from an object using Equation 2.3. The Echo pin has a slight delay from initial transmission, to ensure that the system receives the ultrasonic echo, and not the original transmitted ultrasonic signal. Figure 4.2 shows the timing diagram for the HC-SR04 sensor.

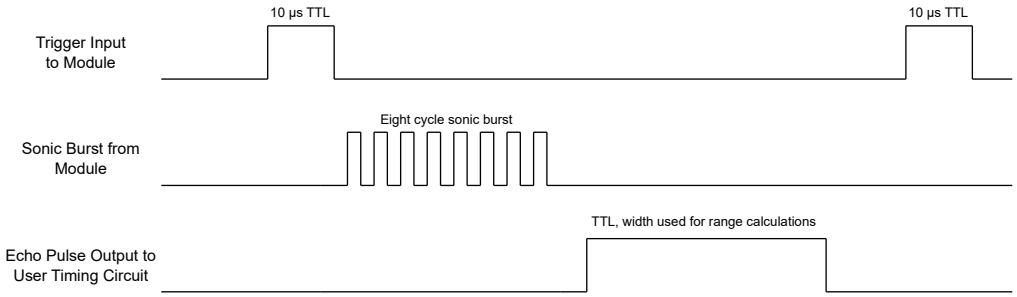

Figure 4.2: HC-SR04 timing diagram, adapted from [39].

4.2.2 Circuit analysis

Documentation relating to the circuit of the HC-SR04 is not publicly available by the manufacturers, therefore it is necessary to reverse engineer the circuit to understand the operation of the HC-SR04 sensor. The HC-SR04 PCB contains three integrated circuits, of which two are unmarked. These devices are labelled as U1, U2 and U3 on the PCB board, of which U1 is marked as a TI LM324 Quad operational amplifier. Using information from previous reverse engineering projects [40, 41, 42], U2 is a one-time programming (OTP) EM78P153A microcontroller, however it is uncertain if the exact IC is used on this version of the HC-SR04 sensor. U3 is a H-bridge IC, which is used to produce two PWM signals of 5V at 40kHz with a duty cycle of 50%, where the PWM signals have a phase offset of 180°. Figure 4.3 shows a circuit diagram of the HC-SR04 PCB. Certain elements of the PCB board have been left out of the circuit diagram, as they do not provide any interesting information i.e. 40kHz piezocrystal Y1 connections to U2. The resistors are marked with their expected impedance, however the capacitors are unmarked. The values

of each capacitor and resistor listed within Figure 4.3 are obtained by removing the components from the HC-SR04 PCB board, and measured using a multimeter. While the expected impedance values of the resistors could be listed instead of their measured values, their measured values are listed to demonstrate the tolerances of the components, and more accurately reflect the operation of the analysed HC-SR04 sensor.

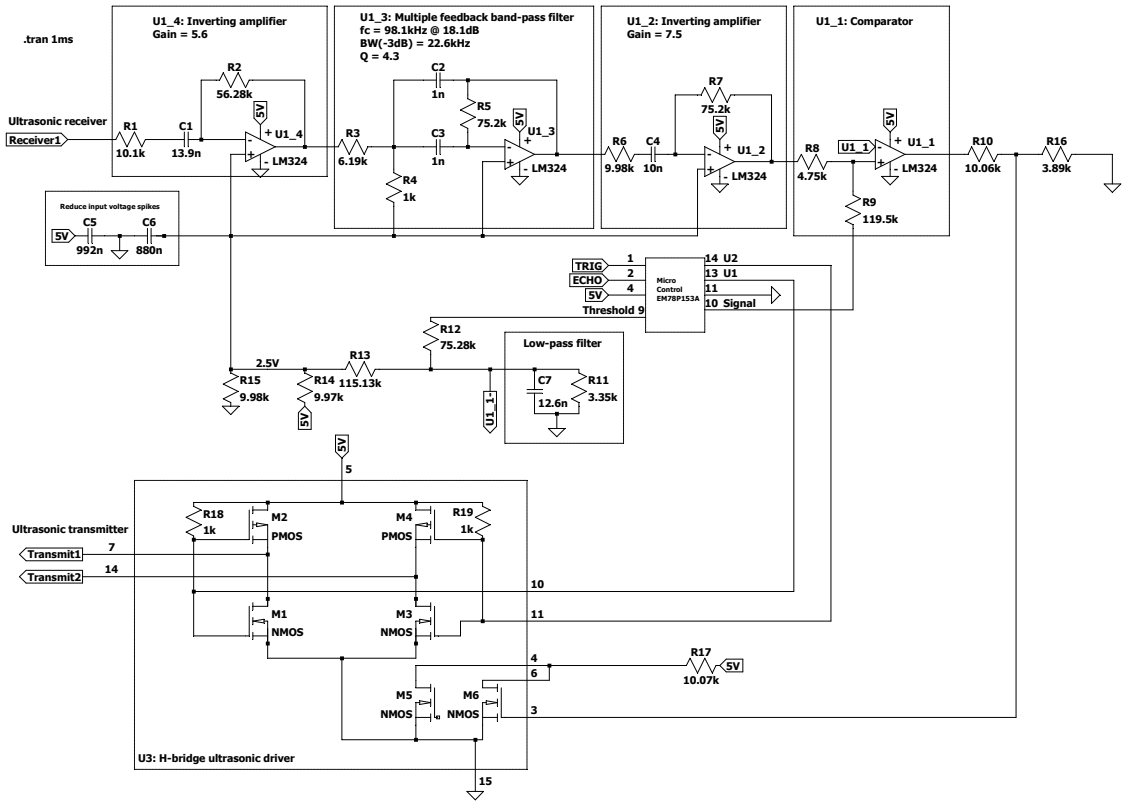

Figure 4.3: HC-SR04 circuit diagram.

The signal processing chain begins with the ultrasonic receiver obtaining an ultrasonic AC burst with a magnitude varying from $800\text{mV}_{\text{p-p}}$ to $135\text{mV}_{\text{p-p}}$. The magnitude will decrease as the distance increases from the target, however this relationship is not used for determining the distance. The ultrasonic burst is connected to an inverting amplifier, U1_4, with a gain of 5.6. The positive input of the inverting amplifier is connected to 2.5V, which is generated from a voltage divider seen at R14 and R15. This increases the magnitude of the received signal, while adding a DC bias which changes the signal from a bipolar signal to a unipolar signal.

The output of U1_4 is connected to a multiple feedback bandpass filter, U1_3. The transfer function of the system can be determined by Equation 4.1 [43].

$$\frac{V_O}{V_{IN}} = \frac{-H\omega_0 s}{s^2 + \alpha\omega_0 s + \omega_0^2} = \frac{-s\dfrac{1}{R3\ C2}}{s^2 + s\dfrac{(C2+C3)}{C3\ C2\ R5} + \dfrac{1}{R5\ C3\ C4}(\dfrac{1}{R3} + \dfrac{1}{R4})} \tag{4.1}$$

For the multiple feedback band-pass filter, this relates to a center frequency f_0 at 18kHz, a maximum gain of 15.6dB, and a Q factor of 6. A simulation of the frequency and phase response of the bandpass filter using LTSpice can be seen in Figure 4.4.

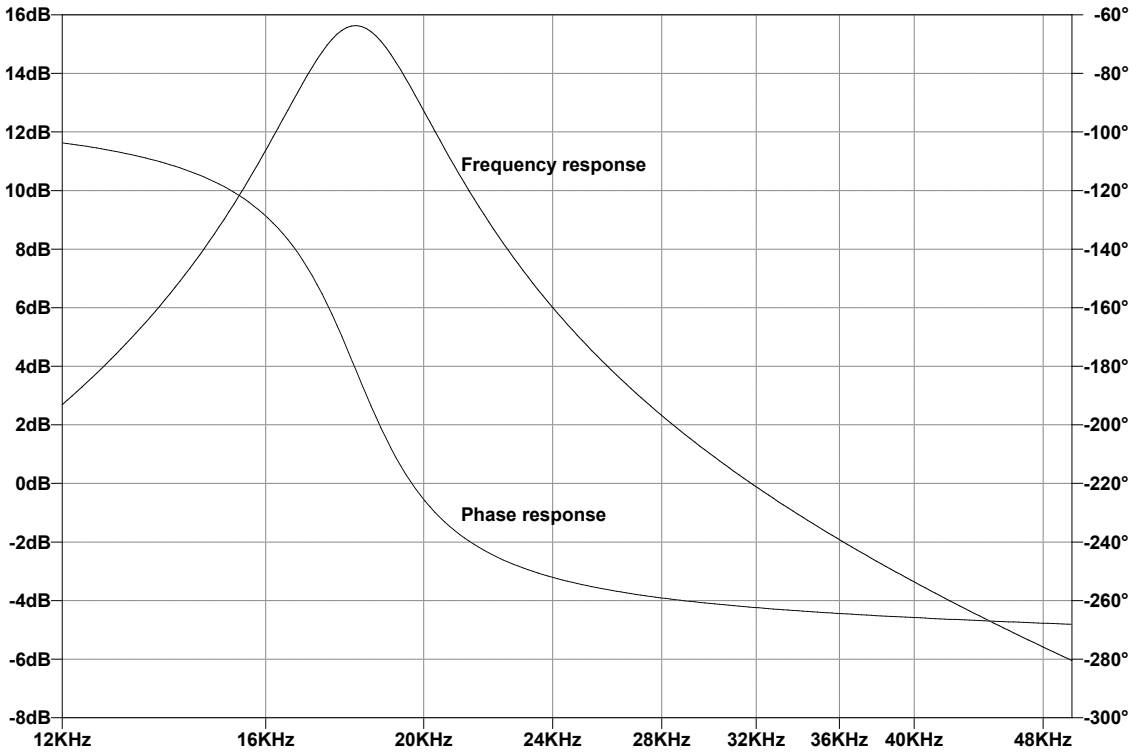

Figure 4.4: Simulated frequency and phase response of HC-SR04 U1_3 multiple feedback band-pass filter, highlighting frequencies of interest.

Considering the frequency of interest is the received 40kHz ultrasonic signal, it is interesting to see that the filter has been designed to attenuate all signals above 32kHz. When comparing the output of U1_4 to U1_3, the output of U3_1 seems to have amplified the middle point of each harmonic, while slightly reducing the power of each harmonic. It is possible that the purpose of the band-pass filter is to redistribute the power of each harmonic to ensure that the largest peak remains at 40kHz.

The output of U1_3 is connected to an inverting amplifier with a gain of 7.5, U1_2. This often causes the output of U1_2 to become clipped at +4V. The output of U1_2 is used as a positive input for a comparator, U1_1. The negative input of U1_1 is set to 2.5V, and begins to discharge and charge every 14.5ms, which is just before the amplitude of the positive input of U1_1 begins to increase and show the ultrasonic signal. The output of U1_1 produces a noisy square wave signal, where the high voltage is +4V, and the low voltage is 2.2V. The positive input of U1_1 is connected in parallel to the microcontroller U2, and the square wave output of U1_1 is used to control the H-bridge ultrasonic driver, U3. Further control signals for the H-bride ultrasonic driver are transmitted from U2, and the transmission and reception cycle continues.

4.2.3 Repurposing the HC-SR04 as an airspeed sensor

The HC-SR04 device control sequence has been designed to function as one cohesive unit, meaning the ultrasonic receiver system will not actively listen if the onboard ultrasonic transmitter has not transmitted an ultrasonic signal. This means that the HC-SR04 is not suitable for applications which require two HC-SR04 sensors facing each other and transmitting an ultrasonic signal back and forth.

The HC-SR04 has been designed to function with a 5V DC power supply, however when checking the technical documentation for each component, all components are capable of operating at 3.3V. The device was tested at 3.3V, but the ultrasonic sensor yielded a distance of 0, regardless of real distance. Using an oscilloscope, it was seen that the HC-SR04 is capable of transmitting a 40kHz ultrasonic signal, and receiving the signal. The sensor yielded a distance of 0, because the received signal voltage levels are too low to trigger the comparator at the negative input of U1_1. This shows that the system can function, if the comparator voltage limits are readjusted to accommodate for the change of supply voltage.

5

Design and Implementation

The purpose of the airspeed sensor is to determine the indicated airspeed of the fixed-wing drone while flying. The velocity of the drone is determined by the superposition of two vectors: the velocity exerted by the drone itself, and the velocity of wind flowing at the drone. Since the drone is a fixed-wing drone, it is forward flying, hence the airspeed sensor is designed to measure the velocity of wind within one axis, which is along the nose and tail of the drone. Harsh turning manoeuvrers may skew the direction of airflow relative to the measurement axis, however this problem will occur with all airspeed measurement devices designed for one axis, such as Pitot tubes. Angular correction algorithms to accommodate for turning manoeuvrers can be developed, but require integration with the entire system, which is outside of the project scope.

The airspeed sensor will use an ultrasonic signal to determine the airspeed of the fixed-wing drone. The ultrasonic device will have a predetermined distance, meaning the purpose of the sensor is to record the change in transmission time with respect to the transmission medium. For an ultrasonic sensor, this means that the temperature, humidity of air, air pressure, and wind will change the speed of sound within the transmission medium. The ultrasonic sensor is interested in recording the effects of wind on the transmission medium, which happens to be the only transmission medium characteristic with a directional component. This implies that the speed of sound will change depending on the direction of transmission relative to the air flow.

This system will provide indicated airspeed recordings, which must be calibrated to provide more accurate airspeed recordings. This requires a calibration process to accommodate for positional errors and instrument errors. Positional errors can be reduced through positioning the airspeed sensor in a location which reduces the presence of wind reflected from the drone body. Instrument errors are inherent to the device, as the ultrasonic airspeed sensor will always come in contact with the freestream, causing distortions within airspeed measurements. Unlike Pitot tubes, the ultrasonic airspeed sensor measures the airspeed close to the drone body, meaning air reflected from the drone body will increase the airspeed measurement error. Since two forms of error exist, the ultrasonic airspeed sensor requires a calibration process while removed from the drone to determine instrument errors, and a second calibration process while attached to the drone to reduce positional errors.

5.1 Design overview

Figure 5.1 shows the overall architecture of the ultrasonic airspeed sensor. The ultrasonic airspeed sensor system is composed of three main systems: the ultrasonic control system, the analog signal processing board, and the ESP32 microcontroller.

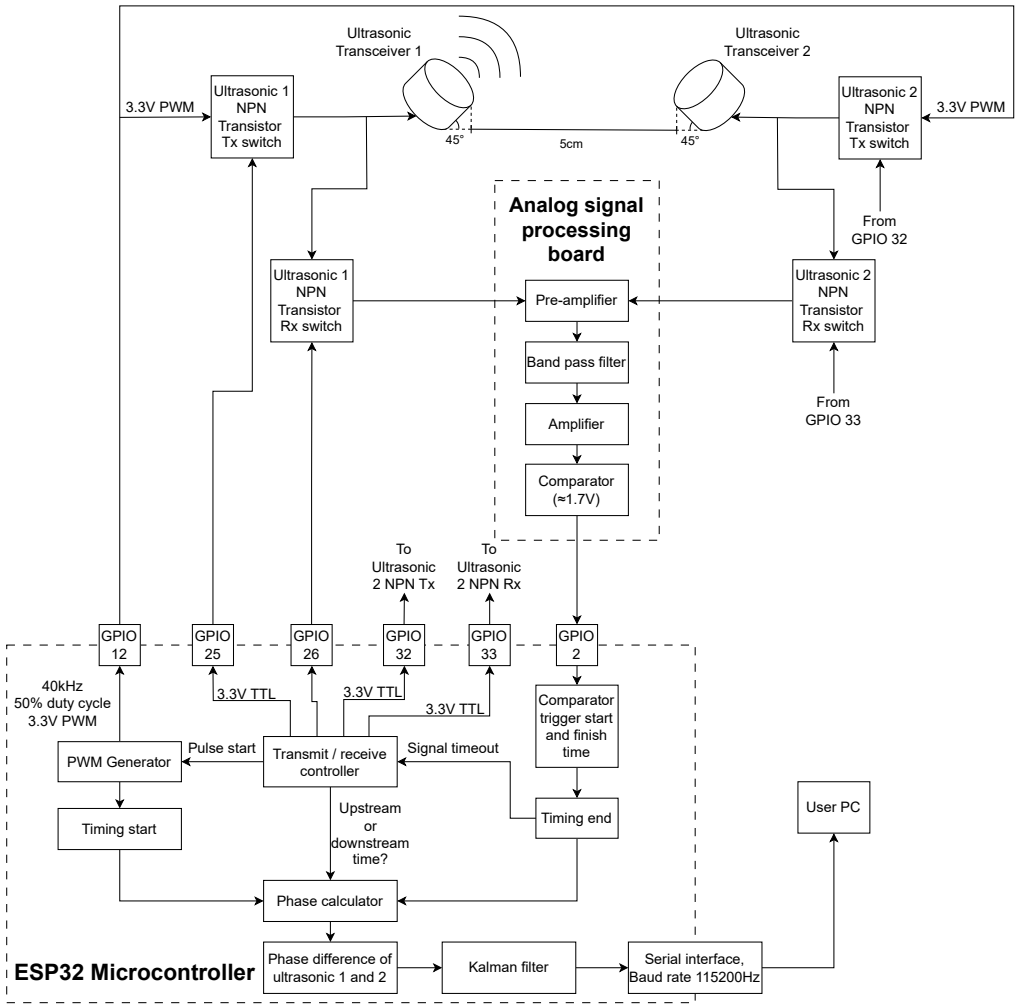

Figure 5.1: Ultrasonic airspeed sensor block diagram.

Likewise to a Pitot-static system, the ultrasonic airspeed sensor will require the total transit time and static transit time to determine the airspeed. The ultrasonic airspeed sensor does not contain a separate static port, meaning the static and total transit time will be determined through two ultrasonic transceivers placed an equal distance apart, close to parallel with the direction of travel. The ultrasonic airspeed sensor will record two transmission times: the upstream and downstream transit times. During flight, upstream transit times will always be longer than downstream transit times, as the flow of wind will act against the drone direction of travel. If the angles of transmission relative to the wind are the same, then the transit time median value will equal the transit time without the effect of wind, or the static

transit time. The difference in static transit time to a transit time will determine the airspeed with respect to the angle of transmission.

The ultrasonic sensor will perform the following steps to obtain an airspeed value:

- Record the ultrasonic transmission time when transmitting at a known angle upstream with respect to air flow.
- Record the ultrasonic transmission time when transmitting at a known angle downstream with respect to air flow.
- Find the median time value of upstream and downstream transmission. The median time will indicate the transmission time without the effects of wind.
- The difference in median transit time to recorded times will indicate the wind velocity with respect to the air angle of attack.
- Apply calibration correction values to accommodate for positional, angular, and instrument errors.

Real-time performance is essential for the operation of the airspeed sensor. Ultrasonic anemometers have an output refresh rate ranging from 1Hz to 32Hz. The output rate of Pitot tubes is substantially higher, producing outputs at 1kHz for low-cost pressure sensors. The ultrasonic airspeed sensor design is focused on developing a middle ground between ultrasonic anemometer accuracy and Pitot tube output rate, while maintaining a low power consumption to ensure longer flight times.

5.2 Ultrasonic transceivers

Ultrasonic transceivers are preferred to separate ultrasonic transmitters and receivers, as having a transducer combined in one package will reduce the weight and size of the ultrasonic airspeed sensor. These devices are considered monostatic, whereas the HC-SR04 system is considered bistatic. One of the main drawback of monostatic transducer topology is that the excitation ringing-decay of the sensor creates a blind zone that limits the minimum detection range [20]. Ultrasonic sensors function by vibrating a piezoelectric device, hence the vibrations must dissipate before an ultrasonic transceiver can take an accurate distance reading. This problem is overcome by the fact that the ultrasonic transceiver within the airspeed sensor does not receive its own signal. This gives the device enough time to dissipate its energy when its role is changing from a transmitter to a receiver.

The ultrasonic transceivers selected for this design are the CUSP-TR80-15-2500-TH ultrasonic transceivers developed by SameSky [48]. These devices are capable of transmitting a 40kHz signal, with a detection range of 15m when operated with $80V_{p-p}$. Performance of the transceiver at voltages below $80V_{p-p}$ is not listed, however a reduced operational voltage will reduce the transmission range and sound pressure level of the ultrasonic piezoelectric. Since the ultrasonic speed sensor does not require a large transmission range, a reduced operational voltage is acceptable.

To get an understanding of the operation of the ultrasonic transceiver, two ultrasonic transceivers are placed 5cm apart. The ultrasonic airspeed sensor should be designed to protrude as little as possible from the drone body, therefore the transceivers are skewed upwards at 45° to create an angle of separation of 90°. The ultrasonic transceivers have a directivity of 80°, meaning the ultrasonic transceivers can be

positioned close to perpendicular to the drone body. This will reduce freestream disturbances caused by the ultrasonic transceivers, which in return improves drone aerodynamics by reducing the profile of the ultrasonic airspeed sensor.

One ultrasonic transceiver is connected to an external waveform generator, where the waveform generator is set to a unipolar 40kHz 3.3V_{p-p} PWM signal with 50% duty cycle. The other ultrasonic transceiver is connected to an oscilloscope and ground, which will act as the receiving ultrasonic transceiver.

5.2.1 Transmission analysis

The expected transmission time is determined by using the time of flight equations established in Section 2.4.1. At a distance of 5cm and setting the speed of sound to 343m/s, an ultrasonic pulse is expected to arrive 145.77μs after initial PWM transmission. Generally, multiple cycles are required to ensure that the oscillations within the ultrasonic transceiver are noticeable. This is because the ultrasonic transceiver needs to continuously oscillate in order to increase the magnitude of the vibrating piezoelectric. Figure 5.2 shows that it takes 1ms for the upstream ultrasonic transceiver to reach its maximum amplitude of 134mV_{p-p} when using the downstream transceiver as a transmitter. From initial PWM transmission to 225μs, the influence of the received ultrasonic signal on the upstream ultrasonic transceiver is not noticeable. A 40kHz PWM cycle has a length of 25μs, meaning that a minimum of three PWM cycles are necessary to produce a noticeable output from the ultrasonic transceiver, and 34 PWM cycles are necessary to reach the maximum amplitude of the ultrasonic transceiver.

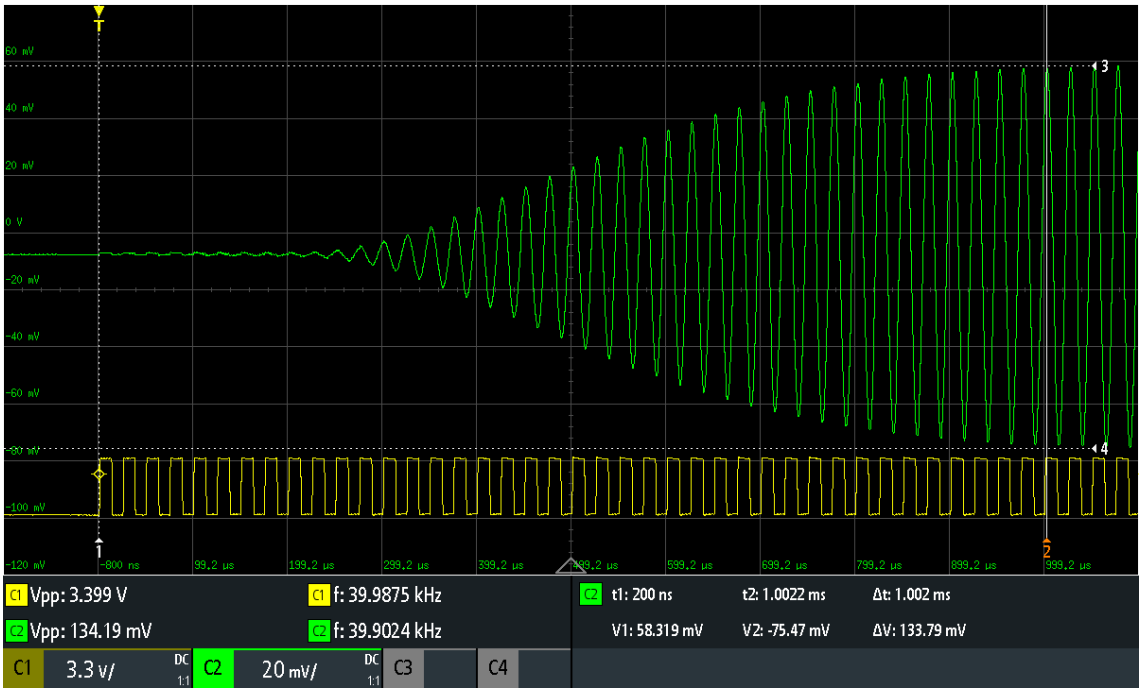

Figure 5.2: Initial measured transmission characteristics of the upstream ultrasonic transceiver. Yellow waveform is the downstream PWM signal, green waveform is the output of the upstream ultrasonic transceiver.

The system uses two ultrasonic transceivers of the same model, but slight difference in performance can be expected between the two devices. Figure 5.3 shows the initial transmission characteristics of the system when the roles of the ultrasonic transceivers are swapped. Likewise to the upstream transceiver, the first ultrasonic pulse is not noticeable within the ultrasonic receiver output, therefore multiple ultrasonic pulses are necessary to generate a change in output voltage. The downstream ultrasonic transceiver reaches a maximum amplitude of 83mV$_{p-p}$ after 700μs.

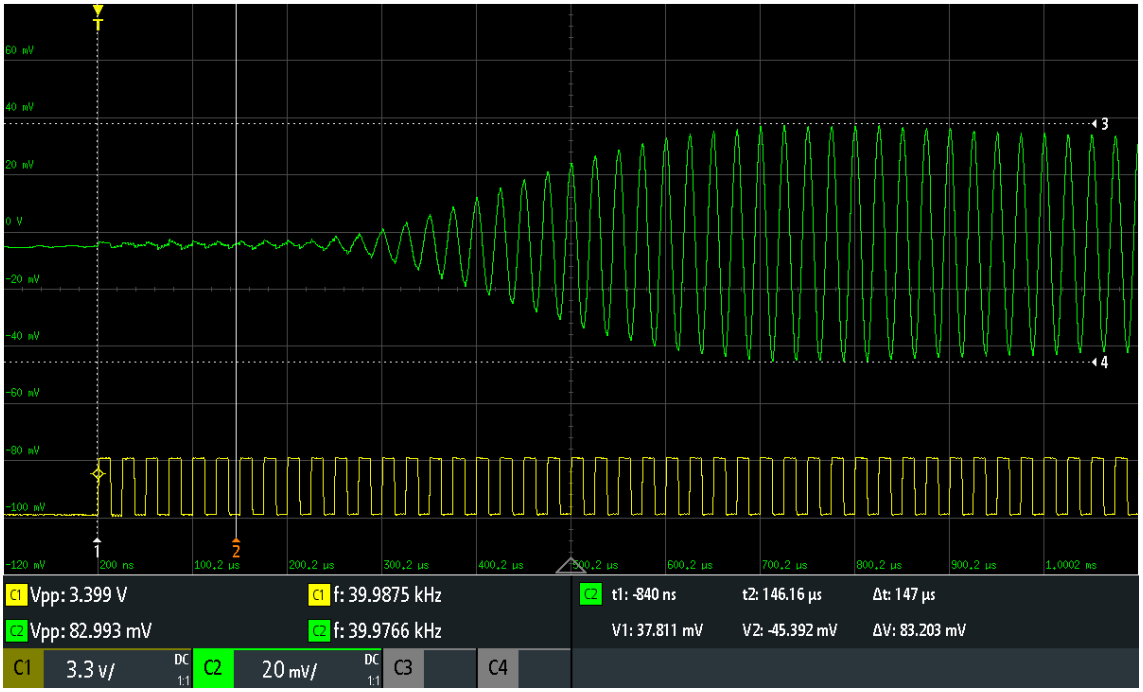

Figure 5.3: Initial measured transmission characteristics of the downstream ultrasonic transceiver. Yellow waveform is the upstream PWM signal, green waveform is the output of the downstream ultrasonic transceiver.

The maximum amplitudes of the ultrasonic transceivers do not match, meaning the system cannot use the time to reach max amplitude as a reference point to indicate the transmission time. This may not create issues when using a comparator based time recording system, as the comparator is typically set to trigger at 70% of the maximum amplitude. This is more likely to create issues for digitising the signal, as a reduced amplitude will not utilise the entire resolution span of an ADC. A potential fix is to match the maximum voltage amplitude of both ultrasonic transceivers using separate amplifier circuits. The maximum voltage amplitude will fluctuate due to the superposition of the wind, therefore it may not be necessary to match their maximum amplitude.

The rate of voltage change due to oscillation is different between both devices: this equates to +0.13mV/μs for the upstream transceiver, and +0.112mV/μs for the downstream transceiver. This shows that the downstream transceiver is lagging, which will introduce a system error that must be considered when recording the transmission times using a comparator based system.

5.3 Ultrasonic analog circuit

The ultrasonic analog circuit consists of two ultrasonic transceivers, an analog signal processing board, and transistor switches. The purpose of this circuit is to propagate an ultrasonic signal from ultrasonic transceiver 1, which is received by ultrasonic transceiver 2. The signal received by ultrasonic transceiver 2 is processed by an analog signal processing board converter board, which removes signals outside of the frequency bandwidth of interest, amplifies the signal, and triggers a comparator set at a pre-determined voltage level.

The comparator will produce a square wave that falls to 0V when the comparator voltage threshold has been exceeded, and rise to 3.3V when the received voltage is lower than the comparator voltage threshold. The voltage level is set to trigger when the waveform is rising, however the exact time that the comparator will trigger is not always known. To accommodate for this, two timestamps are recorded: the first when the input voltage exceeds the comparator voltage threshold, and the second when the input voltage decreases below the comparator voltage threshold. The median value of these two time recordings will indicate the peak of a waveform.

Once a time recording has been obtained, the roles of ultrasonic transceiver 1 and 2 will swap, to determine transit time when transmitting in the opposite direction. Figure 5.4 shows the ultrasonic analog circuit, including the ultrasonic transceivers, control transistors and signal processing circuitry.

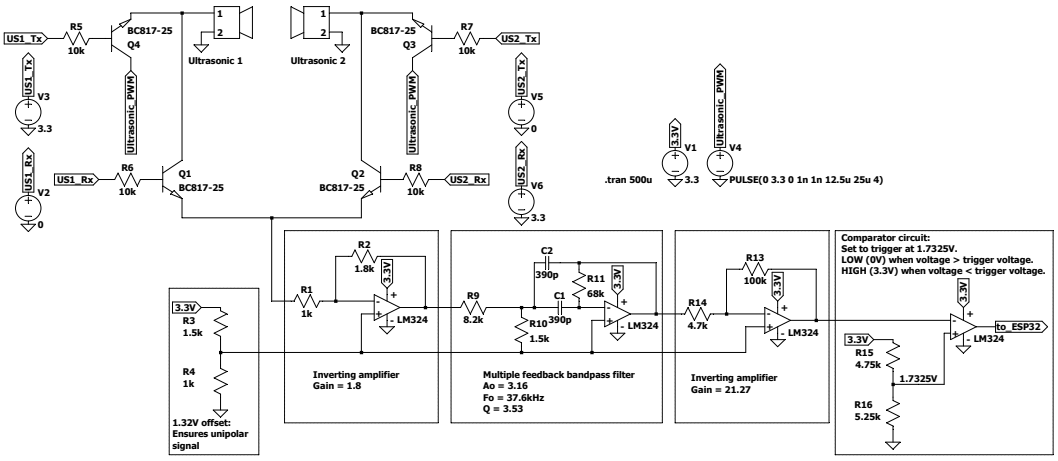

Figure 5.4: Ultrasonic analog circuit design.

The ultrasonic analog circuit is powered by the ESP32 3.3V 600mA power supply. The ESP32 GPIO pins are capable of transmitting 3.3V, where the sum of GPIO currents must be less than 120mA for safe operation. Six GPIO pins are connected to the ultrasonic analog circuit: four for controlling the transistors, one for PWM generation, and one to receive the analog comparator signal. Three extra GPIO pins can be used to communicate with the onboard ADC through an SPI interface.

5.3.1 Control switches

The ultrasonic transceivers contain one signal pin, and a ground pin, meaning that signal pin is continuously connected to the ultrasonic transmission and reception circuit. The control switches are necessary to isolate transmission and reception circuits from each other, allowing for the change of ultrasonic transceiver roles at high speeds. This will reduce the risk of the ultrasonic driving signal from distorting the received ultrasonic signal, as the filtering system will not be capable of separating the two 40kHz signals. The control switches are BC337 BJT NPN transistors, developed by onsemi [49]. These devices are suitable for low-power switching applications, requiring a base-emitter on voltage of 1.2V to turn on, and a current gain bandwidth product of 100MHz. The minimum collector-emitter breakdown voltage is 45V, ensuring that the device can adequately isolate the 3.3V PWM signal. Four NPN control switches are used, and turned on with 3.3V TTL signals coming from the ESP32. PNP transistors were avoided to reduce system complexity, as a negative supply voltage is required for activating PNP transistors.

5.3.2 LM324 operational amplifier

The LM324 quad operational amplifier is used within the analog signal processing chain to develop the necessary filters, and boost the received ultrasonic signal to an appropriate level for processing. With a single supply voltage range of 3V to 36V, and a unity-gain bandwidth of 1.2MHz, these devices are suitable for conditioning the ultrasonic signal. These operational amplifiers are also integrated into the HC-SR04 design, demonstrating that these devices are applicable of ultrasonic processing applications.

Analysing the datasheet of the LM324 shows that when operating at 5V, the LM324 open loop gain at 40kHz is 30dB, and the closed loop gain is at 20dB [50]. These characteristics are important to consider when developing inverters and bandpass filters, as each active component must remain below these values to ensure stability within the circuit. The LM324 package contains four operational amplifiers, allowing for the gain to be spread among multiple amplifiers, ensuring system stability at the cost of increasing system delay.

The operational amplifier cannot produce voltage swings from rail-to-rail, as the maximum voltage output of the op amp is determined by $Vcc - 1.5\text{V}$ [50]. Using a 3.3V power supply, this limits the voltage output to 1.8V. The low level voltage output ranges from 5mV to 20mV. This sets a minimum gain necessary to utilise the full voltage range of the operational amplifier. Considering the ultrasonic transceivers are expected to produce a maximum voltage of $83\text{mV}_{\text{p-p}}$ to $133.8\text{mV}_{\text{p-p}}$, the minimum gain necessary is 22. It is preferable to increase the gain higher than 22 as it will reduce the amount of transmission pulses necessary to receive a detectable signal. Figure 5.4 shows that the received ultrasonic pulse is amplified by a factor of 121. This causes the system to reach its maximum amplitude after 21 pulses, as opposed to 34 pulses as described in Section 5.2.1. The gain can be increased further to reduce the amount of transmission pulses necessary, however it can increase the chance of signal clipping. To prevent the amplification of noise, the majority of amplification occurs after the signal has been filtered.

The fact that the voltage output is limited to 1.8V can create potential issues when creating a comparator to interact with the ESP32. The digital terminal characteristics of the ESP32 [51] show the guaranteed input voltages to trigger a logic level high (V_{HL}) ranges from 0.75Vdd to Vdd + 0.3, and logic level low (V_{IL}) ranges from −0.3V to 0.25Vdd. The ESP32 is powered through a 5V serial connection, however the device steps this down to 3.3V. Therefore, the guaranteed logical level high minimum voltage is 2.475V, and the guaranteed logical level low maximum voltage is 0.825V. The maximum voltage output of the LM324 OpAmp falls outside of the guaranteed logical level ranges, which leaves the ESP32 susceptible to missing comparator triggers, which will cause a cycle of delay within the time recordings. This error can be compensated for through software, as the offset will be a multiple of 25μs.

5.3.3 Bandpass filter

The primary frequency of interest is 40kHz, where all other signals outside of this frequency can be attenuated. Using an oscilloscope, the ultrasonic transceiver receives a 40kHz signal with negligible harmonic power, however a 50Hz hum is present within the signal. This shows that the bandpass filter does not need a tight bandwidth, therefore the bandwidth can be kept large in order to achieve a lower sensitivity, known as a Q factor. To reduce the amount of components necessary, a bandpass filter with an amplification stage is preferred. The multiple feedback bandpass filter was selected for this purpose, which has the same architecture as the bandpass filter used within the HC-SR04 in Section 4.2.2. Figure 5.5 shows the frequency and phase response of the multiple feedback bandpass filter, with a Q factor of 3.53 centred at 37.6kHz.

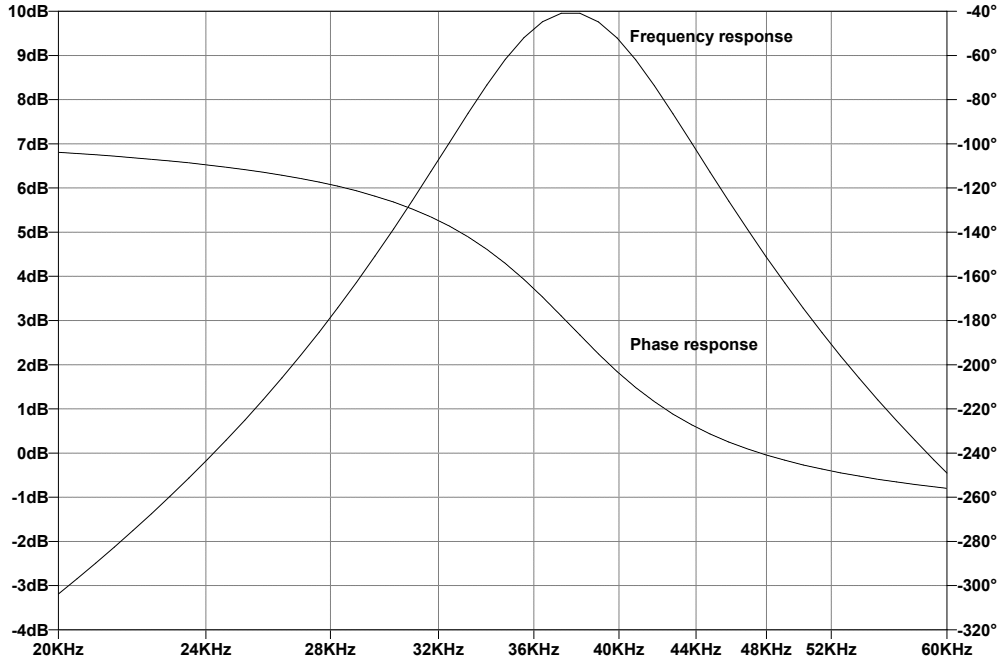

Figure 5.5: Simulated multiple feedback bandpass filter frequency and phase response.

The centre frequency 37.6kHz is somewhat shifted from the desired 40kHz, however a 40kHz signal is still within the bandwidth of interest, and has a gain magnitude 9.3dB, as opposed to the mid-band gain H of 10dB. This difference is acceptable for this specific application, as external signals close to 40kHz are not expected to appear within the received ultrasonic signal. As for the decrease in expected gain, this can be fixed by tuning inverting amplifiers to compensate for this loss.

An important design consideration for the bandpass filter, is the gain bandwidth required to implement the filter. Equation 5.1 is used to obtain the absolute minimum gain bandwidth required from the operational amplifier to implement the filter, where f_c is the centre frequency, Q is the sensitivity of the filter, and A is the gain of the filter. This value is typically multiplied by a factor of 100 to guarantee system stability.

$$f_c \cdot Q \cdot A = GBW_{min} \tag{5.1}$$

For the selected bandpass filter, the minimum gain bandwidth is 420kHz. The gain bandwidth of the LM324 operational amplifier is 1.2MHz, therefore the bandpass filter can be designed using the LM324 operational amplifier.

5.3.4 Analog comparator

An analog comparator is used to indicate that a voltage threshold has been exceeded by the circuit. This device is placed at the end of the ultrasonic signal processing chain, where the threshold voltage is set to trigger when the ultrasonic signal is close to a peak. The time from PWM transmission to comparator triggering is recorded, and used to determine the transmission time of the ultrasonic signal. The comparator will not trigger the instant the first ultrasonic signal reaches the ultrasonic transceiver, as a variety of delays must be accounted for. This includes signal propagation time through the analog circuit, and the ultrasonic signal must be propagated multiple times to produce an oscillation high enough to exceed the voltage threshold. An increase in PWM cycles will increase the ultrasonic signal amplitude, limited by the operating voltage of the transmitting ultrasonic transceiver. With perfect conditions, the number of PWM cycles necessary to exceed the voltage threshold will be the same. When wind is superposed with the transmitting ultrasonic signal, the amplitude of the signal may vary, meaning the number of ultrasonic signals required to exceed the voltage threshold will change.

5.4 ESP32 Microcontroller

The ESP32 serves four purposes within the design: powering the signal processing circuit through 3.3V, generating a 40kHz 3.3V PWM signal for ultrasonic signal propagation, controlling the state of the ultrasonic transceivers, and determining the wind speed through recording the time of upstream and downstream transmission. The ESP32 microcontroller was selected for its high clock speed of 240MHz and low operational voltage of 3.3V.

5.5 Software design

Figure 5.6 shows a block diagram of the software implemented on the ESP32 microcontroller. The design interacts with six GPIO ports, and transmits wind speed recordings to the user PC through a Serial interface. For integration with a flight controller, a SPI interface is preferred, as flight controllers typically expect to interface with devices that communicate through I2C, SPI or CAN.

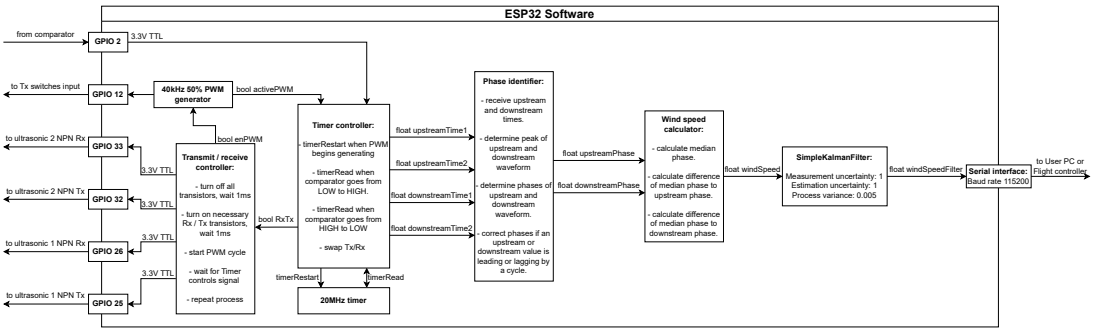

Figure 5.6: ESP32 software block diagram.

5.5.1 Transmit / receive controller

The transmit / receive controller is used to assign the correct signals to the output GPIO ports. This includes transmitting a 3.3V signal to a the corresponding Rx/Tx NPN transistor switches, to ensure that one ultrasonic transceiver is receiving, and the other is prepared to transmit the PWM signal. The controller is transmitting 0V to the NPN transistor switches that should be closed during the transmission cycle, as this prevents the oscillations from the transmitting ultrasonic transceiver from interfering with the receiving ultrasonic signal. Only NPN transistors were selected, as controlling PNP transistors with the ESP32 can cause issues. The minimum voltage that the ESP32 can handle is -0.3V, therefore extra circuitry is required to integrate PNP transistors into the circuit.

The transmit / receive control sequence consists of:

- Switching off all control transistors, and waiting for 1ms. This allows for oscillations within the ultrasonic transceivers to settle, ensuring that previous ultrasonic oscillations do not influence new recordings.
- Switching on the necessary Rx/Tx transistors, depending on if upstream or downstream transmission recordings are required. The system will then wait for 1ms, to allow for system settling.
- Start the PWM cycle, by calling on the 40kHz PWM generator. This will begin transmitting the PWM signal, and the controller will wait a transmission time value has been received.
- Once a transmission time has been received, the controller will repeat the process, but swapping the necessary Rx/Tx transistors that need to be turned on.

5.5.2 Timer controller

The timer controller utilises a 20MHz timer to record the time when the comparator triggers from high to low, and from low to high. The timer controller will restart the 20MHz timer once the PWM has become active, using this as a reference point for transmission time recordings. These values will be used to determine the peak of a received ultrasonic signal, which is passed to the phase identifier for further processing. Once this value has been passed, the timer controller will indicate that the system is ready to obtain a new upstream or downstream recording.

The transmission time will change by 0.42μs if the speed of sound changes by 1m/s. This means that the minimum clock required to record a time difference of 0.42μs is 2.4MHz. To obtain a high degree of accuracy, the clock was increased to 20MHz, allowing for the system to detect speed of sound changes of 0.15m/s.

5.5.3 Phase identifier and wind calculator

The phase identifier take in four inputs: two upstream time values and two downstream time values. These values represent the time that the comparator transitioned from high to low, and low to high in reference to the start of PWM generation. These two values tend to have a time separation less than 6μs, and the comparator is set to transition from high to low during the rise of the received ultrasonic waveform. This indicates that the median time between the two stream values shows the peak of the received ultrasonic waveform.

In an ideal system, the comparator would record the exact time that the first ultrasonic pulse reaches the ultrasonic transceiver. Various delays exist within the system which need to be accounted for in order to retrieve the wind speed, including:

- The ultrasonic piezoelectric requires multiple ultrasonic pulses to oscillate to a detectable voltage level. This will add a delay of 25μs per PWM cycle.
- The rate of voltage change to pulses is different between the two devices, as outlined in Section 5.2.1: this means that even without the influence of wind, the upstream and downstream time recordings will have an offset depending on the amount of ultrasonic cycles transmitted.
- The ultrasonic signal needs to propagate through the signal processing board before arriving to the ESP32. Delays caused by electronic components must be considered.
- The ultrasonic transceiver will begin oscillations from 0V, as the piezoelectric vibrations are sinusoidal. The comparator records the peak of the waveform, meaning the transmission time must be reduced by half a cycle, 12.5μs.

A simpler approach can be used, where the phases of the upstream and downstream recordings can be cross-correlated to determine the influence of wind on transmission times. The method uses the displacement of upstream phase to downstream phase to determine the airspeed of the drone. This method does not need to account for intrinsic delays within the system, but further calculations are necessary to accommodate for PWM cycle offsets. Calculating the airspeed using a phase-based system will limit the time detection difference to half a cycle, 12.5μs. If we consider 343m/s as the speed of sound centre point and the ultrasonic transceiver distance of separation is 5cm, the ultrasonic airspeed sensor should be calibrated

to ensure that the transmission time centre point is 145.77μs. This allows for the device to record transmission times of $145.77 \pm 12.5\mu$s, which relates to a speed of sound range of 315.9m/s to 375.178m/s. This allows the device to record airspeeds of $\pm$29.63m/s, if the speed of sound without wind superposition remains constant. Further calculations are required to accommodate for the influences of temperature, humidity and pressure on the speed of sound.

5.5.4 Kalman filter

A Kalman filter functions as a mean squared error minimiser, reducing errors within wind speed measurements by accommodating for statistical noise and reducing the effects of inaccuracies by producing estimated wind speed values in relation to previous results. An extended form of a Kalman filter is integrated into the ArduPilot sensor firmware, allowing for the flight controller to fuse all available data to determine vehicle position, velocity and angular orientation [53]. Sensor fusion data of interest for the ultrasonic airspeed sensor includes accelerometers, GPS, compass and gyroscope information, allowing for the system to obtain more accurate airspeed measurements when integrated within the full system. The ultrasonic airspeed sensor is developed as a stand-alone product, therefore availing of the ArduPilot Extended Kalman Filter is not within the scope of the thesis. To evaluate the effectiveness of the Kalman filter on ultrasonic airspeed measurements, a simple Kalman filter for 1-D information is used [52].

Three parameters are selected through the simple Kalman filter [52]:

- Measurement uncertainty: this represents how much the measurement is expected to vary. This has been set to 1m/s.
- Estimation uncertainty: an initial value representing how much uncertainty is expected within the Kalman filter estimation. This has been set to 1, however this value is dynamically adjusted as more estimates are produced by the Kalman filter.
- Process variance: how fast the measurement moves. For the Simple Kalman Filter Library, this value ranges from 0.001 to 1, with 0.001 indicating slow measurement movement. This value has been set to 0.005.

A low process variance value provides stability to the system, at the cost of reducing the rate of change of wind speed measurements. This can cause the system to miscalculate wind speed measurements during turbulent flight, as gusts of wind or rapidly changing wind conditions may not be reflected in the filtered wind speed measurements.

6
Results

This section presents results obtained through static testing and wind testing. Static testing is used to demonstrate the performance of the system through oscilloscope signal analysis, and the stability of the system through a long running test in a wind-free environment.

Wind testing was performed to analyse the accuracy and precision of the system under controlled wind velocities, and to analyse the system characteristics of the ultrasonic airspeed sensor under rapidly changing wind conditions. Accuracy and precision testing is performed in a semi-closed loop wind tunnel, provided by Chalmers Laboratory of Fluids and Thermal Science. Rate of change testing is performed using a hairdryer, as the wind tunnel is not capable of producing instantaneous changes in wind conditions.

Accuracy refers to how close the measured value of a sensor is to the true quantity. Equation 6.1 is used to determine the accuracy of the sensor measurement, where V_{meas} is the measured value, V_{true} is the true value, and V_{range} is the total range of the sensor. The target measurement range is 0m/s to 25m/s, however the current device has a predicted range of -12.5m/s to 12.5m/s. Both methods equate to a V_{range} of 25m/s.

$$\text{Accuracy} = \frac{|V_{meas} - V_{true}|}{V_{range}} \cdot 100 \tag{6.1}$$

Precision refers to the consistency and repeatability of a sensor's measurement. This is determined by analysing the variation of sensor results when measuring the same quantity repeatedly. Equation 6.2 is used to determine the precision of the system as a percentage, where σ is the standard deviation, and $\bar{x}$ is the mean. Assuming the sensor data follows a normal distribution, the standard deviation is doubled to obtain a confidence interval of 95%.

$$\text{Precision}(\%) = (\frac{2\sigma}{\bar{x}}) \cdot 100 \tag{6.2}$$

6.1 Ultrasonic waveform analysis

Figure 6.1 shows the full operation of the ultrasonic airspeed sensor with each control state labelled. Three waveforms of interest were recorded with the oscilloscope: the yellow waveform is the comparator output, the green waveform is the received ultrasonic signal as seen at the comparator negative input, and the orange waveform

is the PWM signal from the ESP32. The output rate of the system is recorded as 200Hz.

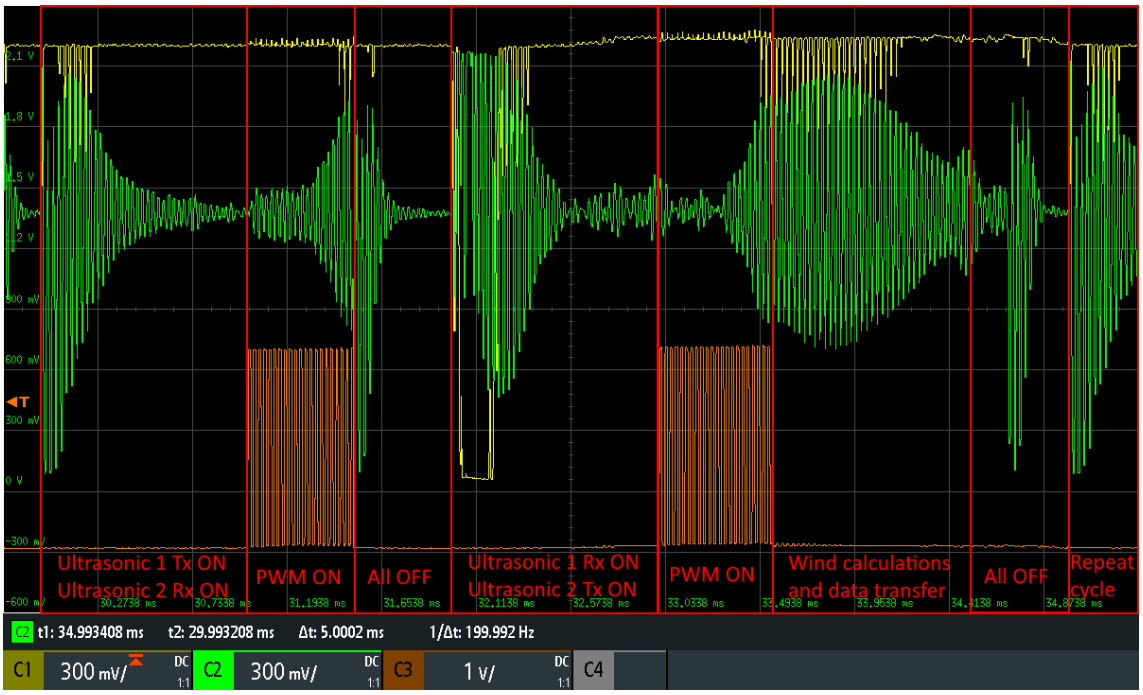

Figure 6.1: Measured full operation cycle of the ultrasonic airspeed sensor with states labelled. The yellow waveform is the comparator output, the green waveform is the negative comparator input, and the orange waveform is the PWM signal.

Turning on and off transistors causes voltage spikes within the system, which has been accommodated for by adding delays to the system to allow the voltage spikes to ring out. It is crucial to let the system voltage dissipate before ultrasonic transmission, as it prevents noise from corrupting the received ultrasonic signal.

Another source of noise which affects the received ultrasonic signal is the PWM transmission signal. During the time that the PWM is active, a small portion of the signal ripples through the signal processing board, appearing as a 40kHz $0.4V_{p-p}$ sinusoidal signal with a DC offset of 1.32V. The PWM signal is transmitted to both Tx transistors, however only one Tx transistor is turned on at this time. The closed transistor is not capable of blocking the entire PWM signal, and the filtering system is not capable of removing noise with a frequency of 40kHz. The comparator voltage threshold needs to be raised higher than this noise, ensuring that the comparator triggers at a time where the received ultrasonic signal is the dominant signal within the signal processing board.

Figure 6.1 shows that the system receives the downstream ultrasonic signal as a 40kHz $1.4V_{p-p}$ sinusoidal signal with a DC offset of 1.32V. The comparator currently triggers at 90% of the maximum amplitude, which ensures that the ultrasonic signal is the dominant signal, and allows for a margin of error for cases where the superposition of wind causes the maximum amplitude to fluctuate.

Data transfer and wind speed calculations occur after the upstream and downstream values have been recorded. The time gap between upstream and downstream

recordings is kept to a minimum, as harsh weather conditions can cause the wind to rapidly change. Increasing the time gap between recordings can produce outdated measurements, therefore it is crucial to keep this time period as short as possible.

6.2 System stability with no wind

Figure 6.2 compares the wind speed readings of the ultrasonic airspeed sensor before and after using the software Kalman filter in real time during a static test. The purpose of the Kalman filter is to reduce the influence of measurement noise on real-time airspeed measurements: a clear example of spurious readings can be seen by the sharp increase of unfiltered airspeed measurements from -0.12m/s to 2.25m/s. The Kalman filter is still capable of reacting to the spurious readings, however their influence on airspeed measurements is reduced by a factor of ten.

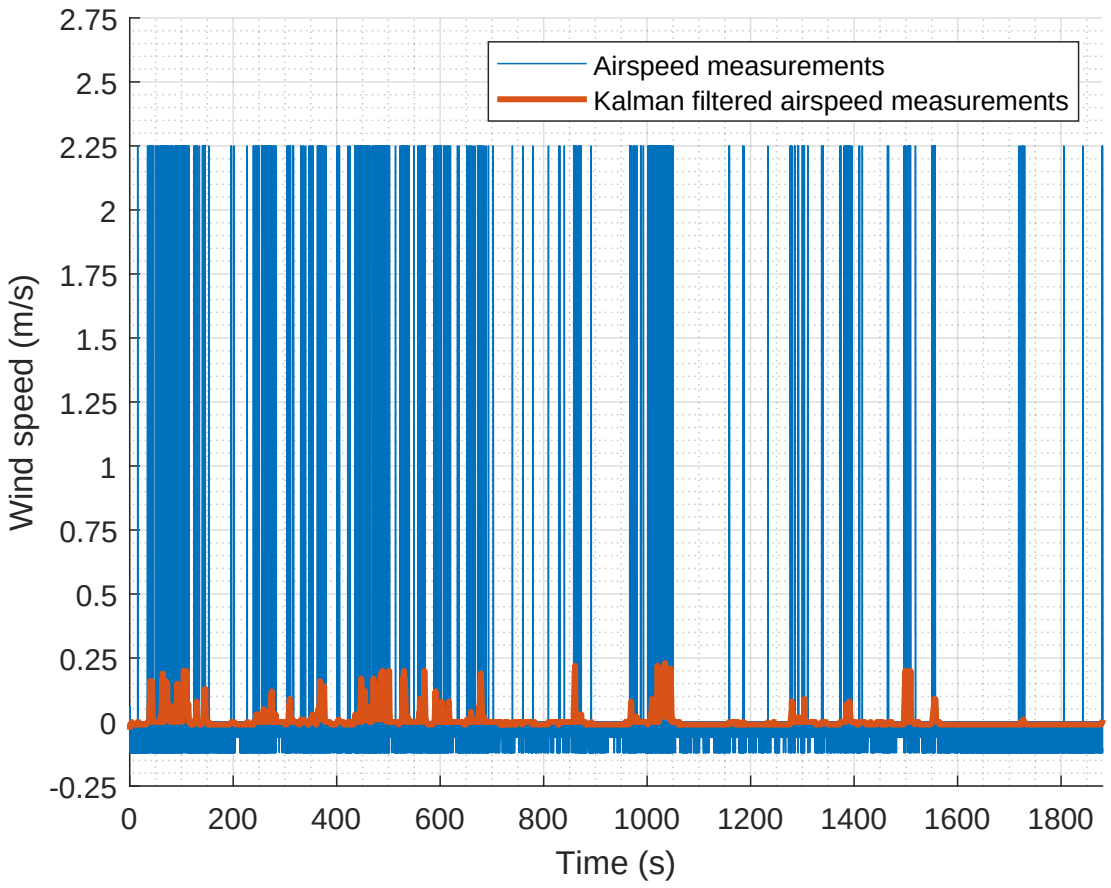

Figure 6.2: Measured ultrasonic airspeed values under static conditions.

Table 6.1 highlights key information seen in Figure 6.2, while comparing the mean accuracy and precision of the two systems. From Table 6.1, it is clear that digital filtering systems are necessary to produce more accurate airspeed measurements.

	Unfiltered airspeed	Kalman filtered airspeed
Maximum airspeed (m/s)	2.25	0.23
Mean airspeed (m/s)	0.0056	0.0028
Minimum airspeed (m/s)	-0.12	-0.03
Mean accuracy	0.0224%	0.0112%
Precision (m/s)	±2.244	±0.2972

Table 6.1: Comparison of unfiltered and Kalman filtered airspeed measurements during static testing.

6.3 System response to instantaneous wind

The purpose of the instantaneous wind test is to get an understanding of the response time of the ultrasonic airspeed sensor. The Kalman filter process variance and measurement uncertainty variable can be tuned to increase or decrease the response time of the system, at the cost of increasing potential errors within the system. Figure 6.3 demonstrates the response of the system when using a hairdryer to produce an instant source of wind. Two speeds and directions are tested, to obtain an understanding of the systems performance within a rapidly changing environment.

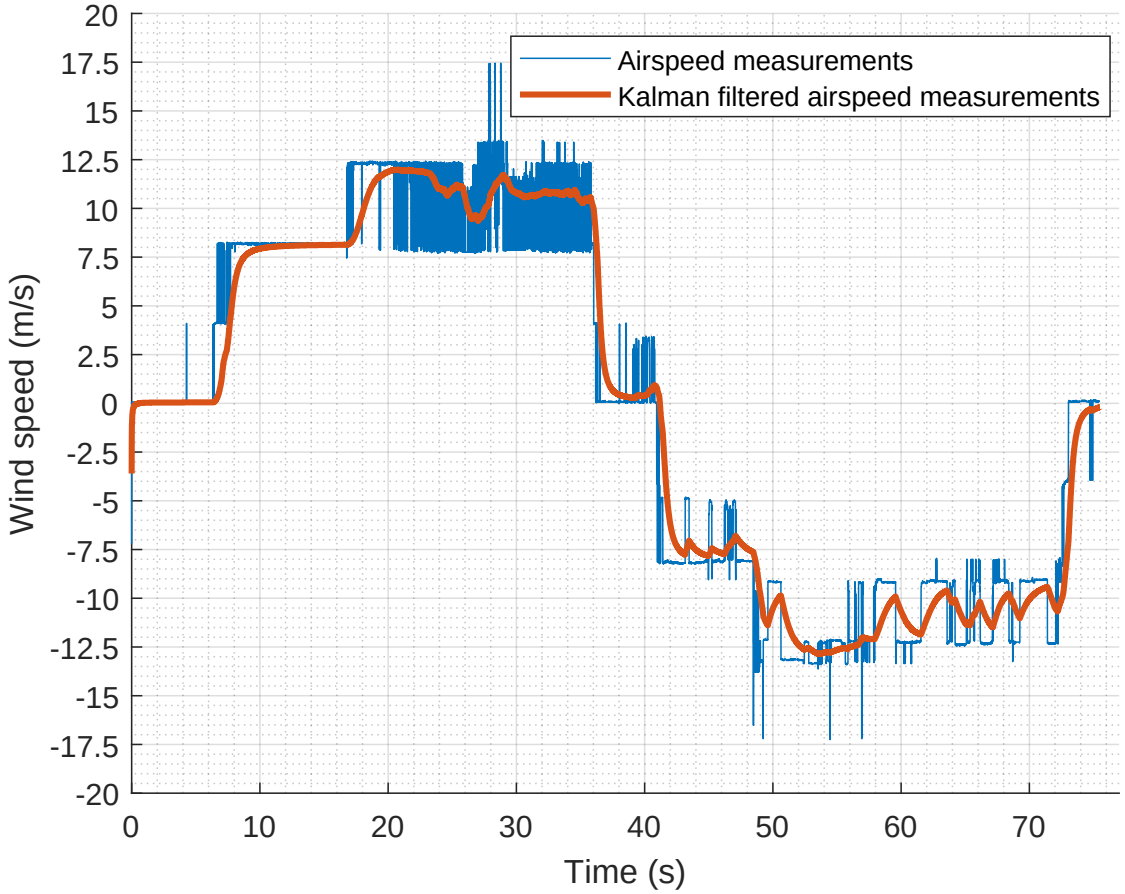

Figure 6.3: Measured time-velocity graph, demonstrating the influence of an instantaneous wind source on system performance.

The response of the ultrasonic airspeed sensor shares similarities to a linear first-order differential system: the Kalman filter does not overshoot or oscillate when reaching its target measurement value, and the relationship between the speed of sound and wind superposition is a first-order differential equation.

A notable characteristic of a first-order system is the rise time, which is defined as the time it takes for an output to rise from 10% to 90% of its final value. Multiple rising and falling sections exist within Figure 6.3, the first of which is the rise from 0.06m/s to 8.1m/s. Figure 6.4 presents the rise in question, highlighting the start co-ordinate (6.375s, 0.06m/s), end co-ordinate (13.025s, 8.1m/s), 10% co-ordinate (6.895s, 0.8m/s) and 90% co-ordinate (8.515s, 7.24m/s).

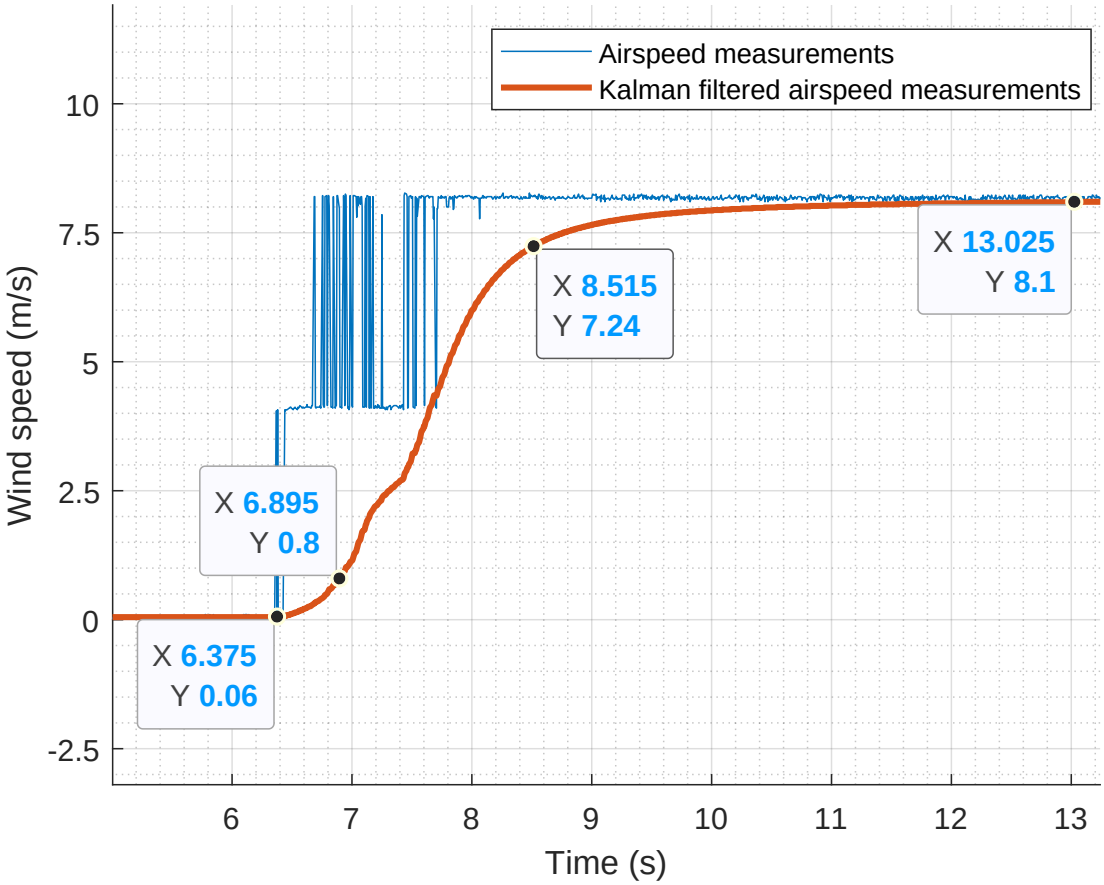

Figure 6.4: Calculating the rise time of the Kalman filtered results, with values of interest labelled.

Equation 6.3 uses the values obtained from Figure 6.4 to obtain the rate of change of the system. Using co-ordinates $(X_{90\%}, Y_{90\%})$ = (8.515s, 7.24m/s) and $(X_{10\%}, Y_{10\%})$ = (6.895s, 0.8m/s), Equation 6.3 produces a rate of change of 3.975m/s^2.

$$\frac{Y_{90\%} - Y_{10\%}}{X_{90\%} - X_{10\%}} = \text{Rate of change} \tag{6.3}$$

This process is repeated across multiple rises and falls to determine the rate of change. This has produced a range of values, from 1.63m/s^2 to 7.122m/s^2, showing

that the relationship between the rate of change is non-linear and reliant on the precision of the unfiltered ultrasonic airspeed recordings.

6.4 Wind tunnel testing

The ultrasonic airspeed sensor was tested using a wind tunnel, which provides a controlled wind environment for evaluating the airspeed measurements. Figure 6.5 shows an error bar graph, comparing the results of the ultrasonic airspeed sensor to a control wind velocity. The bar represents the maximum and minimum recorded airspeed, where the circled value on the bar represents the mean airspeed measurement. The control wind ranged from 5m/s to 15m/s in steps of 2.5m/s. The minimum airspeed measurement recording time was 203s, allowing for the system to obtain a minimum of 40600 samples. The main area of interest is from 10m/s to 12m/s, as this is the stalling speed range of the fixed-wing drone.

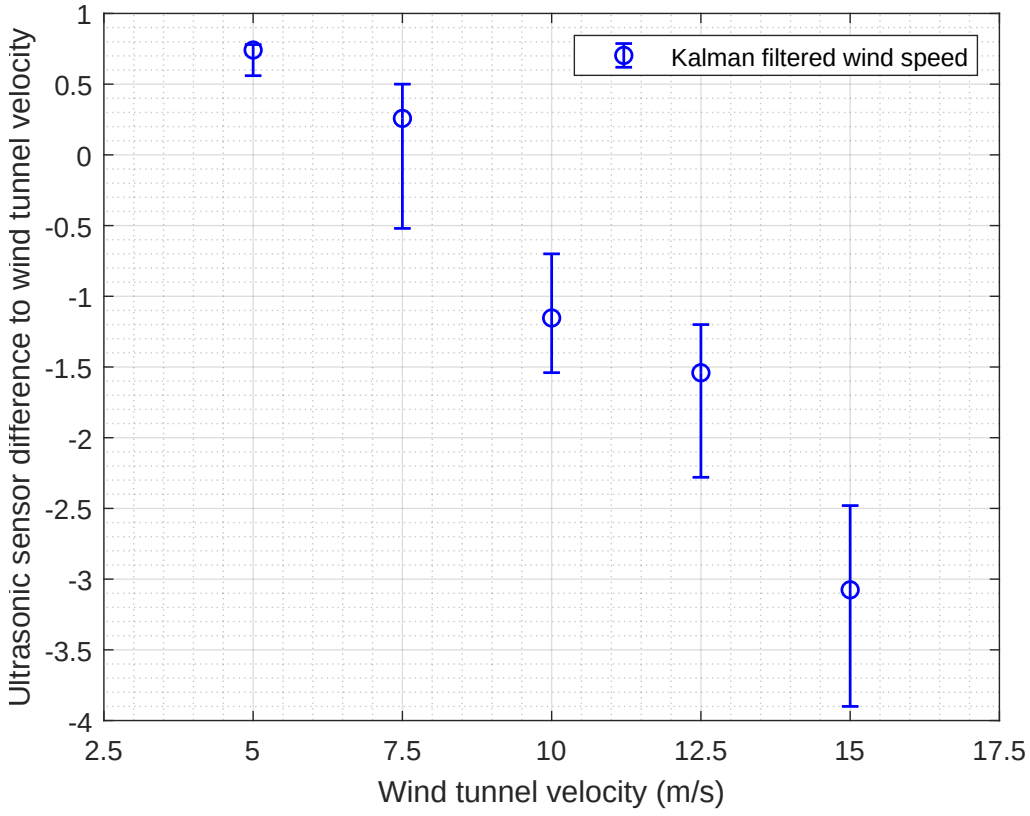

Figure 6.5: Error bar graph, demonstrating the measured difference in ultrasonic airspeed readings to wind tunnel velocity.

The system functions to a high degree of precision at 5m/s, where the minimum and maximum recording range is 0.2m/s. The mean airspeed has an offset of 0.24m/s demonstrating that further calibration to accommodate for measurement offsets is still required. The performance of the ultrasonic airspeed sensor begins to decrease as the velocity increases. The maximum error occurs at 15m/s, where the mean airspeed has an offset of -3.1m/s, where maximum and minimum values have a

range of 1.42m/s. This error makes the ultrasonic airspeed sensor incapable of providing accurate data during critical flight speeds, showing that the device requires further calibration before reliable data can be produced. Table 6.2 shows the key findings of the wind tunnel test.

Wind tunnel velocity (m/s)	5	7.5	10	12.5	15
Maximum airspeed (m/s)	5.78	8	9.3	11.3	12.52
Mean airspeed (m/s)	5.741	7.757	8.84	10.95	11.924
Minimum airspeed (m/s)	5.56	6.98	8.46	10.22	11.1
Mean accuracy, 25m/s range	2.96%	1%	4.6%	6.2%	12.3%
Standard deviation, 2σ	0.0858	0.4148	0.3988	0.3194	0.8086
Precision, 2σ, 95% confidence	1.5%	5.35%	4.5%	3%	6.8%

Table 6.2: Wind tunnel testing of the ultrasonic airspeed sensor.

6.5 Power demands

To analyse the impact of integrating the ultrasonic airspeed sensor on the flight time of a drone, the power demands of the sensor must be established. This is determined through measuring the current and voltage of the system during operation. The calculations used to establish power demands will make the following assumptions:

- All GPIO ports from the ESP32 to the ultrasonic airspeed sensor printed circuit board produce a consistent 3.3V. This includes all the four transistor control GPIO ports, the PWM GPIO port, and the $3.3V_{DC}$ power supply.
- The current is measured in series from ESP32 GPIO ports to the airspeed sensor printed circuit board using a multimeter. This will obtain an average current reading during operation. Current spikes that may occur during transition of states are not considered.
- Power demands of the ESP32 are not considered, as the ESP32 is not optimised for the ultrasonic airspeed sensor. The ESP32 contains Bluetooth, radio and WiFi modules [51] which are not necessary for the ultrasonic airspeed sensor, but may still draw power when inactive. If these components are inactive, the ESP32 is considered in Modem Sleep mode, which consumes 3mA to 20mA of current [55].

Table 6.3 shows the current draw from each ESP32 GPIO port connected to ultrasonic airspeed sensor PCB. The multimeter allows for the selection of DC, AC and AC+DC current detection, providing three different values for each GPIO port. US1 and US2 represents ultrasonic transceiver 1 and 2 respectively, Tx represents the transmission control transistor, and Rx represents the receiving control transistor.

Current source	DC	AC	AC+DC
3.3V supply pin (mA)	1.97	0.04	1.97
US1 Tx GPIO 25 (mA)	0.180	0.125	0.130
US1 Rx GPIO 26 (mA)	0.023	0.071	0.072
US2 Tx GPIO 32 (mA)	0.038	0.108	0.112
US2 Rx GPIO 33 (mA)	0.098	0.066	0.116
PWM GPIO 12 (mA)	−0.221	0.43	0.476
Total current (mA)	2.97	0.84	2.877

Table 6.3: ESP32 multimeter current measurements during operation.

The supplied voltage to the PCB is 3.3V, therefore the power demands of the system averages at 9.5mW when considering the combined AC and DC current measurements. Other than the 3.3V power supply pin, GPIO 12 consumes the most power at 1.57mW. GPIO 12 is used to generate the PWM signal to drive the ultrasonic transceiver, where a high power consumption is required in order to generate enough pressure within the ultrasonic piezoelectric.

The LM324 operational amplifier requires a quiescent current of 240μA per amplifier when powered with a 5V supply voltage [50]. The datasheet does not list the quiescent current of the device when supplied with 3.3V, therefore it is assumed that the real quiescent current is close to 240μA. As all four amplifiers are in use, the LM324 requires 0.96mA when the device is enabled, but inactive. Comparing this to Table 6.3, the LM324 consumes 33% of the total power within the system when it is inactive. This value will increase depending on the current of the signal as it passes through the signal processing circuit.

6.5.1 Power demands on battery lifespan

Drone batteries are typically measured in quantity of cells (S), and milliampere-hours (mAh). For lightweight drones, this ranges from four to six cells and 1000mAh to 1500mAh. Equation 6.4 is used to determine the battery lifespan, where $I_{capacity}$ is the milliampere-hours of the battery, and I_{load} is the current load applied to the battery.

$$\text{Battery life hours} = \frac{I_{capacity}(\text{mAh})}{I_{load}(\text{mA})} \tag{6.4}$$

With a battery charge of 1000mAh, the ultrasonic airspeed sensor can stay powered for 105 hours under ideal conditions. This value will decrease depending on temperature, battery quality and if the battery is powering other devices.

7
Discussion

This section will discuss the performance of the ultrasonic airspeed sensor in reference to the target specifications outlined in Section 1.1, and in reference to the commercially available products discussed in Section 1.3.

7.1 Design specification

Section 1.1 establishes that the goal of the project is to create an ultrasonic airspeed sensor with a measurement resolution of ±0.25m/s, measurement range of 0m/s to 30m/s, and a minimum output rate of 20Hz.

7.1.1 Output rate

The output rate of the ultrasonic airspeed sensor is 200Hz, achieving the set design goal. The output rate of the system can be increased by shortening the stages listed in Figure 6.1. Reducing the time of transistor turn off and turn on states is the simplest way to increase the output rate. The delay between transistor state changes is determined by the ring-out effect of the ultrasonic transceiver and signal processing system. For now, a conservative estimate of ring-out time is used, ensuring that interference does not occur within the system due to previous transmission feedback. A decrease in state change times will not have a knock-on effect on other sensor characteristics, if the ultrasonic sensors are still given the appropriate time to ring-out. Other methods of increasing the output rate include increasing the PWM signal voltage to increase the ultrasonic receiver rate of change, or decreasing the ultrasonic transceiver distance of separation. These methods are not ideal, as a change in one characteristic will influence other system characteristics, such as increasing the system power demands, or increasing the influence of air reflections on airspeed measurements.

7.1.2 Resolution

At the given distance of 5cm, a 20MHz clock is capable of achieving a theoretical airspeed resolution of ±0.15m/s. This has been demonstrated in Figure 6.5, where the airspeed sensor was capable of maintaining a precision of ±0.11 at 5m/s. This achieves the target design goal of ±0.25m/s, however this is only applicable to airspeed measurements of 5m/s and below. For airspeeds 7.5m/s and above, the average precision of airspeed measurements was ±0.5m/s, showing that the system can be improved further through a more extensive calibration process.

7.1.3 Measurement range

Considering only the phase of the received ultrasonic signal limits the airspeed measurement range to detect maximum transmission time differences of $\pm 12.5\mu$s, in conditions where the temperature is stable. This can be achieved by tuning the ultrasonic airspeed sensor to produce phase results of 180° at zero wind conditions. Using Equation 7.1 is used to establish the time measurement range of ultrasonic airspeed system, where d is the distance of transceiver separation, t_{static} is the time of transmission under no wind conditions, and 12.5μs is half the period of the 40kHz ultrasonic signal.

$$\frac{d}{t_{static} \pm 12.5\mu\text{s}} = \text{Time range} \tag{7.1}$$

If we consider the speed of sound at zero wind conditions to be 343m/s and the distance of separation is 5cm, the transmission time is 145.77μs. Using Equation 7.1, the ultrasonic airspeed sensor can measure from 315.9m/s to 375m/s, meaning it can calculate airspeed measurements of ± 27.1m/s. The target measurement range is from 0m/s to 30m/s, showing that the device is slightly under the target maximum airspeed. The range can be improved by using a different method that focuses on the frequency of the signal, or a more traditional time of flight calculation which accounts for system delays to obtain the true time of arrival. These methods can be used in conjunction with the current method to obtain more accurate and precise airspeed measurements.

7.1.4 Power consumption

The ultrasonic airspeed sensor PCB requires 9.5mW. This value does not consider the power requirements of the ESP32, where the current draw in Modem Sleep mode ranges from 3mA to 20mA. The ESP32 can be powered by a regulated $5V_{DC}$, which converts the voltage to 3.3V. Other methods of powering the device exist, but these typically bypass onboard voltage regulators. Regardless of powering method, the ESP32 requires a $3.3V_{DC}$ power supply. This means the power requirements for the ESP32 ranges from 10mW to 66mW.

The power consumption can be compared to a Pitot-static system recommended by ArduPilot, which is the Holybro DroneCAN airspeed sensor, which integrates a DLVR-L10D digital pressure sensor built for ArduPilot based systems [56]. This device operates with 5V, and requires a 100mA current source. This means the full system has a power requirement of 0.5W, which is significantly higher than the ultrasonic system with the ESP32.

A more fair comparison is analysing the DLVR-L10D pressure sensor by itself. The DLVR-L10D can operate at 3.3V with a typical current requirement of 3.5mA, resulting in a power demand of 11.5mW. Compared to the ultrasonic airspeed PCB's power demand of 9.5mW, the power demands of the DLVR-L10D is still higher.

7.2 Future work

This section will discuss aspects of the ultrasonic airspeed sensor that have been considered during the design process, but not fully explored due to time limitations.

7.2.1 Non-constant speed of sound

The phase-based cross correlation method of calculating the airspeed is limited to 315.9m/s to 375.178m/s, where the speed of sound at room temperature 343m/s is selected as the measurement middle point. This allows for the device to read airspeed differences of 27m/s, but is based off the assumption that the speed of sound is not influenced by static transmission medium characteristics. Without the superposition of wind, the speed of sound can differ from 325m/s to 355m/s, depending on relative humidity and temperature. When operating at $-10°C$, the speed of sound without the influence of wind is 325m/s, meaning the airspeed sensor range is limited to 9m/s.

7.2.2 Flight controller integration

Integration of the ultrasonic airspeed sensor to a flight controller system will require the removal of the ESP32 microcontroller from the system, and the addition of extra IC components to fulfil the duties of the ESP32. This will require all controls, PWM generation and calculations to occur on the analog signal processing board, where the following changes should be implemented to the system:

- 40kHz H-bridge driver for PWM generation.
- Onboard microcontroller IC for receiving comparator results, transistor switch controls, calculating the airspeed through upstream and downstream results, and communications to onboard and offboard devices, such as the flight controller.
- Removal of the Kalman filter from the microcontroller software: ArduPilot fuses sensor data through an Extended Kalman filter, therefore an extra Kalman filter may not be necessary.

A more suitable microcontroller for integration is the PIC32MX250F128D microcontroller by Microchip Technology [58]. This device has a maximum clock speed of 50MHz, two 32-bit timers, control interfaces for SPI and I2C, and a 10-bit 1.1Msps ADC module. The microcontroller requires a voltage between 2.7V to 3.6V with a typical dynamic current draw of 0.5mA/MHz. Likewise to the ESP32, this microcontroller may be excessive, therefore it should be used as a starting point to understand how to integrate an onboard microcontroller to the ultrasonic airspeed sensor system.

7.2.3 Wind dynamic simulations

The closer the airspeed sensor is integrated to the drone body, the higher chance of disruptions within the freestream caused by air reflections. Increasing the distance of separation between the ultrasonic transceivers and drone body will allow the sensor

to record the freestream, however the transceivers themselves will cause air reflections, leading to inaccurate results and an increase of drag. All these factors should be considered to determine an optimal distance, which balances the influences of air reflections on measurements, and drag on aerodynamics and power consumption. This optimal distance can be found using computational fluid dynamics, where a model of the drone and ultrasonic airspeed sensor can be analysed with respect to wind flow.

7.2.4 Analog to digital converter

The analog signal processing board was originally developed to condition the signal for digitisation. The proposed analog to digital converter is the MCP3202 2.7V dual channel 12-bit A/D converter by Microchip. Since the MCP3202 is powered by a $3.3V_{DC}$ supply voltage, the sampling rate of the device will be lower than 80ksps, producing an aliased version of the signal. The usage of an ADC was inspired by common ultrasonic system architectures, as described in Figure 2.1. The idea was to digitise the signal to perform more accurate time of flight calculations: this could be done by identifying the time where the dominant signal transitions from the PWM signal to the received ultrasonic signal. This point in time can be identified by the increased rate of voltage change that occurs when the ultrasonic signal has been received.

The addition of an ADC provides the potential of utilising the Doppler shift effect to determine the airspeed. This can be used in combination with time of flight calculations to record the airspeed with a higher degree of accuracy, as it allows the system to focus on multiple aspects of the received waveform.

This idea was not fully implemented to the system due to time limitations and complexity. The Doppler effect is influenced by the particles per million present within the transmission medium: this is what Doppler effect based ultrasonic flow meters rely on [21]. In terms of an airspeed sensor, this means that air chemical composition and humidity will have an influence on the Doppler effect, introducing errors to the system. To compensate for this, the humidity of air must be known, which requires an additional sensor.

The MCP3202 is not optimal for the purpose of analysing ultrasonic signals, due to the low sampling rate of the system when operating at 3.3V. An alternative ADC designed for ultrasonic signals is the ADS7046 12-bit 3-MSPS SAR ADC by Texas Instruments [59].

7.3 Project planning reflections

This section discusses the process of developing the ultrasonic anemometer in reference to the predicted time plan outlined within the planning report. The time plan has been summarised as a Gantt chart in Figure 7.1.

Thesis week	W1	W2	W3	W4	W5	W6	W7	W8	W9	W10	W11	W12	W13	W14	W15	W16	W17	W18	W19	W20
Date	20.01	27.01	3.02	10.02	17.02	24.02	3.03	10.03	17.03	24.03	31.03	7.04	14.04	21.04	28.04	5.05	12.05	19.05	26.05	2.06
TASK																				
Planning report & meetings																				
Backgroud research																				
Reverse engineering HC-SR04																				
Drone airflow simulations																				
Ultrasonic distance and angle of separation testing																				
ADC board development																				
Controls & pulse reconstruction VHDL software																				
VHDL filter development																				
Simple testing and results analysis																				
Performance comparison of different filter types																				
Standalone wind tunnel testing and results analysis																				
Wind tunnel testing as attached to the drone																				
Presentation preparation																				
DEADLINES																				
Planning report			7.02																	
Preliminary halftime report												11.04								
Halftime report														25.04						
Preliminary report																		23.05		
Report to opposition																				6.06

Figure 7.1: Planning report summarised to a Gantt chart

The objective of the project was to develop an alternative design to the ultrasonic airspeed sensor developed in [15]. This alternative design would be based on the HC-SR04 hardware, and focus on the usage of digital filters implemented on an FPGA. The new design would be compared to the initial prototype, and a comparison of digital filtering methods would be discussed. The location of the prototype ultrasonic airspeed sensor is known, however it could not be retrieved at the time of conducting this project.

The first delay encountered within the project occurred towards the end of the reverse engineering task. The initial idea was to utilise the hardware found on the HC-SR04 sensor. The HC-SR04 contains one ultrasonic receiver and one ultrasonic transmitter, with all control systems within the HC-SR04 accounting for this. During the background research task, it was concluded that the usage of ultrasonic transceivers is preferred. This would reduce circuit complexity, and decrease the number of ultrasonic components necessary. By swapping to ultrasonic transceivers, the HC-SR04 PCB could not be utilised, therefore development of the control and signal processing board was necessary. This process created a significant delay within the project, which caused a knock-on effect with other tasks within the project.

The idea of the ADC board was to perform signal conditioning on the received ultrasonic pulse before it is digitised by the ADC. An ADC was selected to allow for the creation of more complex airspeed measurement algorithms. Both the comparator and ADC method was developed in parallel to allow for a comparison between both methods of airspeed measurement calculations. The ADC and an appropriate SPI interface was developed to extract digitised information, however due to time limitations, this aspect of the project was left underdeveloped.

The ESP32 was initially selected as a testing platform for the ultrasonic airspeed sensor while the FPGA software was being developed. Due to integration issues and time limitations, the usage of the FPGA was removed from the project, and the ESP32 was used as the primary programming platform.

Other aspects of the project that were not completed, but originally planned for, include:

- Airflow simulations of the target drone and the ultrasonic airspeed sensor.
- Performance comparison of different filter types.

- Wind tunnel testing as attached to the drone.

The initial plan was overly ambitious, with the major downfall being the assumption that the HC-SR04 hardware could be repurposed to create an ultrasonic airspeed sensor with minimal adjustments. This assumed that the majority of the workload would consist of FPGA integration and testing, with the intention of completing the hardware by week nine. In reality, the electronic components to develop the signal processing board were received in week ten, providing little time for FPGA integration and the testing of multiple filtering systems.

7.4 Ethical considerations

The origin of drones is tied to the defence and security industry, with the first pilotless vehicle being developed during the First World War [57]. The drone industry has grown within recent years, and continues to grow rapidly during times of warfare. This has caused drone technologies to become a controversial research topic, which is understandable considering that in 2016, 70% of the drone market is dedicated towards military activities [16]. The ethical and societal concerns relating to the development of military-origin technology is complicated, especially when the technology is still actively used by defence and security organisations.

The sole purpose of the thesis is to develop a device which supports search and rescue missions conducted by the Swedish Sea Rescue Society. This thesis has no intention on creating a product for the benefit of military applications, but the risk of research being used for military purposes will always exist.

The usage of generative artificial intelligence (AI) has been avoided as much as possible during this project. Unavoidable interactions with generative AI have occurred during this project, such as being provided with an AI summary by a search engine or writing suggestions from generative AI tools which are enabled by default. These features have been ignored or disabled when possible. They have had no influence on the design of the ultrasonic airspeed sensor or on the writing of this thesis.

8

Conclusions

This thesis has explored the potential of applying an ultrasonic anemometer design methodology to develop an ultrasonic airspeed sensor for a fixed-wing drone. The ultrasonic airspeed offers potential advantages over a standard Pitot-static system, such as improved performance under harsh conditions, reducing mechanical components and reduced aircraft drag, however the proposed ultrasonic airspeed sensor performance is not capable of replacing a commercially available Pitot-static system as of yet.

The device is capable of recording indicated airspeed values with an accuracy of 95% for airspeeds less than 10m/s. Further testing is required to provide calibrated airspeed measurements for airspeeds greater than 10m/s, as the operating speeds of the target fixed-wing drone is above 10m/s to prevent stalling.

This thesis focuses on one ultrasonic anemometer design methodology for developing an ultrasonic airspeed sensor. While this design does not satisfy the original design requirements, a wide variety of alternative designs exist. Frequency analysis, coded modulation, and phase lock loops have all been utilised to provide more accurate wind measurements. The usage of ultrasonic signals for measuring wind speeds is well established, however their application for aircraft technologies is still an open question.

Bibliography

[1] W. S. Aiken, "Standard Nomenclature for airspeeds with tables and charts for use in calculation of airspeed", National Advisory Committee for Aeronautics, Langley Field, Virginia, Sep. 1946. Accessed: Apr. 14, 2025 [Online]. Available: https://ntrs.nasa.gov/api/citations/19930081759/downloads/19930081759.pdf

[2] Sjöräddningssällskapet, sjoraddning.se, https://www.sjoraddning.se/ (accessed Jul. 02, 2025)

[3] Joint Committee for Guides in Metrology, *"Guide to the Expression of Uncertainty in Measurement"*, bipm.org. https://www.bipm.org/en/committees/jc/jcgm/wg/jcgm-wg1-gum (accessed May 25, 2025)

[4] A. Suryana, M. A. S. Yudano, "Ultrasonic Sensor for Measurement of Water Flow Rate in Horizontal Pipes Using Segment Area" in *Fidelity: Jurnal Teknik Elektro*, vol. 5, pp. 60-68, 2023

[5] S. K. Ammann, "Ultrasonic anemometer", United States Patent number US5343744A, Sep. 6, 1994

[6] B. Pincent, P. Journe and G. Brugnot, "Ultrasonic anemometer", United States Patent number US4890488A, Jan. 2, 1990

[7] I. A. Kuncara, J. E. Suseno, S. Agus and I. Gunadi, "Development of Ultrasonic Anemometer Using HC-SR04 with Kalman Filter Based on Microcontroller Integated IoT" in *E3S Web Conference*, vol. 202, 2020

[8] A. Haseeb and R. Asim, "Ultrasonic Anemometer Design and Testing in Wind Tunnel", U.S. Agency for International Development, 2019

[9] R. Kawahara, K. Ogwara and H. Shingin, "Airspeed measurement using ultrasonic waves for micro UAVs (in Japanese)" in *Transactions of the JSME (in Japanese)*, vol. 86, no. 887, 2020.

[10] Honeywell, "TruStability® Board Mount Pressure Sensors", 50099533-A-EN GLO, Aug. 2014. [Online]. Available: https://docs.rs-online.com/acd6/A700000008056279.pdf.

[11] Sensirion, "ASP1400 Bidirectional Differential Pressure Meter", V2.1, Jul. 2011. [Online]. Available: https://sensirion.com/media/documents/51693FFE/6183D647/Sensirion_Differential_Pressure_Datasheet_ASP1400.pdf.

[12] ClimaTec, "CYG-81000/81000RE 3-component ultrasonic anemoemter (in Japanese)", weather.jp. https://www.weather.jp/products/wind/sat/cyg-81000/ (accessed Jul. 02, 2025).

[13] V. Soldatkin, V. Soldatkin, G. Sokolova, A. Nikitin and E. Efremova, "Building, Forming and Processing of Signals of the Electronic Sensor Airspeed Vector's

Parameters of Unmanned Aircraft Plane." in *Electromechanics and Robotics. Smart Innovation, Systems and Technologies*, vol. 232, pp. 475-485, 2021

[14] H. Inokuchi, "Aircraft ultrasonic airspeed sensor (in Japanese)", Japanese Patent number JP3574814B2, Mar. 29, 2000.

[15] H. Male, "An ultrasonic airspeed sensor prototype for a fixed-wing drone", Master's thesis, Chalmers University of Technology, 2023.

[16] F. Castellano, "Commercial Drones Are Revolutionizing Business Operations", toptal.com. `https://www.toptal.com/management-consultants/market-research-analysts/drone-market` (accessed May 2, 2025)

[17] W. Gracey, "Measurement of Aircraft Speed and Altitude", *National Aeronautics and Space Administration*, Hampton, Virginia, NASA Reference Publication 1046, May 1980

[18] "Meaurement of airspeed in light aircraft - certification requirements", *Australian Government Civil Aviation Safety Authority*, Advisory Circulat AC 21-40v1.1, Nov. 2022

[19] R. Motte, "Pitot/Static Problems", avaiationsafetymagazine.com. `https://aviationsafetymagazine.com/instrument_flying/pitot-static-problems/` (accessed Apr. 14, 2025).

[20] M. Toa, A. Whitehead, "Ultrasonic Sensing Basics", *Texas Instruments*, Application Note SLAA907D, Dec. 2021

[21] "Doppler Meters Vs Transit Tie Ultrasonic Flow Meters", *Dwyer Instruments, LLC.*, `https://www.dwyeromega.com/en-us/resources/dif-between-doppler-transit-time-ultrasonic-flow-meters` (Accessed 2025-03-19)

[22] FT Technologies, "Unmanned seaplane: Japan." `https://web.archive.org/web/20240528083954/https://fttechnologies.com/case-studies/unmanned-seaplane-uses-ultrasonic-airspeed-sensor/` (Accessed 2025-03-17)

[23] FT Technologies, "FT205 Lightweight Acoustic Resonance Wind Sensor", A4302-1-EN, Jun. 2017. [Online]. Available: `https://www.unmannedsystemstechnology.com/wp-content/uploads/2017/07/FT205-Wind-Sensor-Datasheet.pdf`.

[24] *Ultrasonic Anemometer 1D Instruction for Use* (2022), Adolf Thies GmbH & Co KG, Göttingen, Germany. Accessed: Mar. 20, 2025. Available: `https://www.thiesclima.com/db/dnl/4.386x.xx.xxx_US-Anemometer-1D_e.pdf`

[25] K. G. Panda, D. Agrawal, A. Nshimiyimana and A. Hossain, "Effects of environment on accuracy of ultrasonic sensor operates in millimetre range", *Perspectives in Science*, vol.8, pp. 574-576, June 2016.

[26] V. Nicolau, C. Miholca and M. Andrei, "Fuzzy Rules of Sound Speed Influence on Ultrasonic Sensing in Outdoor Environments", *2009 3rd International Workshop on Soft Computing Applications*, Szeged-Arad, Romania, 2009, pp.145-150, doi: 10.1109/SOFA.2009.5254862. © 2009 IEEE.

[27] C. Pearson, "High-Speed, Analog-to-Digital Converter Basics", Texas Instruments, Application Report SLAA510, Jan. 2011. Accessed Apr. 08, 2025. [Online]. Available: `https://www.ti.com/lit/an/slaa510/slaa510.pdf`

[28] W. Kester, "Undersampling Applications", in *Practical Analog Design Techniques*. Analog Devices, 1995.

[29] S. W. Smith, "Filter Comparison", in *The Scientist and Enginee's guide to Digital Signal Processing*, California Technical Publishing, 1999, ch. 21.

[30] M. Saul, "Benefits of a Delta-Sigma ADC with Programmable FIR and IIR Filters", Texas Instruments, Application Note SBAA587, Sep. 2023. Accessed Apr. 08, 2025. [Online]. Available: https://www.ti.com/lit/ab/sbaa587/sbaa587.pdf

[31] National Instruments, "IIR Filters and FIR Filters", ni.com. https://www.ni.com/docs/en-US/bundle/diadem/page/genmaths/genmaths/calc_filterfir_iir.htm (accessed Jun. 02, 2025)

[32] T. Lacey, *Tutorial: The Kalman Filter*, ch. 11. Massachusetts Institute of Technology, 1998.

[33] Analog Devices, "LTspice", analog.com. https://www.analog.com/en/resources/design-tools-and-calculators/ltspice-simulator.html (accessed Jun. 27, 2025).

[34] Analog Devices, "Analog Filter Wizard", tools.analog.com. https://tools.analog.com/en/filterwizard/ (accessed Apr. 18, 2025).

[35] MathWorks, "Control System Toolbox", mathworks.com. https://mathworks.com/products/control.html (accessed Jun. 27, 2025).

[36] Autodesk, "Autodesk Fusion", autodesk.com. https://www.autodesk.com/products/fusion-360/overview (accessed Jun. 27, 2025).

[37] Prusa Research a.s., "PrusaSlicer 2.9.2", prusa3d.com. https://www.prusa3d.com/page/prusaslicer_424/ (accessed Jun. 27, 2025).

[38] Arduino, "Arduino IDE 2.3.6", arduino.cc. https://www.arduino.cc/en/software/ (accessed Jun. 27, 2025).

[39] *Ultrasonic Ranging Module HC-SR04*, ElecFreaks. Accessed: Mar. 20, 2025. Available: https://cdn.sparkfun.com/datasheets/Sensors/Proximity/HCSR04.pdf

[40] D. Pilling, "HC-SR04", davidpilling.com. Accessed: Mar. 20, 2025. [Online.] Available: https://www.davidpilling.com/wiki/index.php/HCSR04

[41] "Making a better HC-SR04 Echo Locator", uglyduck.vajn.icu. Accessed: Mar. 20, 2025. [Online.] Available: https://uglyduck.vajn.icu/ep/archive/2014/01/Making_a_better_HC_SR04_Echo_Locator.html

[42] D. Abreu Rodríguez, J. Toledo, B. Codina, A. Suárez, "Low-Cost Ultrasonic Range Improvements for an Assistive Device" in *Sensors*, vol. 21, 2021

[43] H. Zumbahlen, "Multiple Feedback Band-Pass Design Example", Analog Devices, 2023. Accessed: Mar. 20, 2025. [Online]. Available: https://www.analog.com/media/en/training-seminars/tutorials/mt-218.pdf

[44] H. Wurzburg and J. Arjun, "Sensor Drivers", ardupilot.org. https://ardupilot.org/dev/docs/code-overview-sensor-drivers.html (accessed Apr. 12, 2025).

[45] M. Usach, "SPI Interface", Analog Devices, Application Note AN-1248, Sep. 2015. Accessed Apr. 12, 2025. [Online]. Available: https://www.analog.com/media/en/technical-documentation/app-notes/an-1248.pdf

[46] T. Brand, "Isolated SPI Communication Made Easy", Analog Devices, Jul. 2019. Accessed Apr. 12, 2025. [Online]. Available: https://www.analog.com/en/resources/technical-articles/isolated-spi-communication-made-easy.html

[47] PuTTY, "PuTTY", putty.org. https://www.putty.org/ (accessed Jun. 27, 2025).

[48] SameSky, "Model: CUSP-TR80-15-2500-TH. Description: Ultrasonic Sensor", Rev. 1.02, Dec. 2024. [Online]. Available: https://www.sameskydevices.com/product/resource/cusp-tr80-15-2500-th.pdf (accessed Jul. 02, 2025).

[49] Onsemi, "NPN Epitaxial Silicon Transistor", BC337-FSC/D datasheet Rev. 3, Apr. 2024. [Online]. Available: https://www.onsemi.cn/download/data-sheet/pdf/bc337-fsc-d.pdf (accessed Apr. 14, 2025).

[50] Texas Instruments, "LMx24, LMx24x, LMx24xx, LM2902, LM2902x, LM2902xx, LM2902xxx Quadruple Operational Amplifiers", SLOS066AD, Sep. 1975 [Revised Oct. 2024]. [Online]. Available: https://www.ti.com/lit/ds/symlink/lm324.pdf (accessed May 26, 2025).

[51] Espressif Systems, "ESP32 Series", Datasheet Version 4.9, Aug. 2016 [Revised Apr. 2025]. [Online]. Available: https://www.espressif.com/sites/default/files/documentation/esp32_datasheet_en.pdf (accessed Apr. 14, 2025).

[52] D. Sene, "Simple Kalman Filter Library", github.com. https://github.com/denyssene/SimpleKalmanFilter (accessed May 28, 2025)

[53] ArduPilot Dev Team, "Extended Kalman Filter (EKF)", ardupilot.org. https://ardupilot.org/copter/docs/common-apm-navigation-extended-kalman-filter-overview.html (accessed May 28, 2025)

[54] R. Michallick, "Application Design Guidelines for LM324 and LM358 Devices", Texas Instruments, SLOA277B, Jan. 2019 [Revised Jul. 2023]. [Online]. Available: https://www.ti.com/lit/an/sloa277b/sloa277b.pdf

[55] Last Minute Engineers, "Insight Into ESP32 Sleep Modes & Their Power Consumption", lastminuteengineers.com. https://lastminuteengineers.com/esp32-sleep-modes-power-consumption/ (accessed Jun. 04, 2025).

[56] HolyBro, "High Precision DroneCAN Airspeed Sensor - DLVR", holybro.com. https://holybro.com/products/high-precision-dronecan-airspeed-sensor-dlvr (accessed Jun. 04, 2025).

[57] Imperial War Museums, “A Brief History of Drones”, iwm.org.uk. https://www.iwm.org.uk/history/a-brief-history-of-drones (accessed Jun. 30, 2025).

[58] Microchip Technology Inc, "PIC32MX250F128D", microchip.com https://www.microchip.com/en-us/product/pic32mx250f128d (accessed Jun. 04, 2025).

[59] Texas Instruments, "ADS7046 12-Bit, 3-MSPS, Single-Ended Input, Small-Size, Low-Power SAR ADC", SBAS785, Dec. 2017. [Online]. Available: https://www.ti.com/lit/ds/symlink/ads7046.pdf.

DEPARTMENT OF MICROTECHNOLOGY AND NANOSCIENCE
CHALMERS UNIVERSITY OF TECHNOLOGY
Gothenburg, Sweden
www.chalmers.se

CHALMERS
UNIVERSITY OF TECHNOLOGY